Universidade do Minho
Escola de Engenharia

Ana Catarina Freitas Salazar de Oliveira

Immobilization of Specific Growth Factors from Platelet Lysate at the Surface of Electrospun Nanofibers for Tissue Engineering Applications

outubro de 2013

Immobilization of Specific Growth Factors from Platelet Lysate at the Surface of Electrospun Nanofibers for Tissue Engineering Applications
Ana Catarina Freitas Salazar de Oliveira
UMinho | 2013

Universidade do Minho
Escola de Engenharia

Ana Catarina Freitas Salazar de Oliveira

Immobilization of Specific Growth Factors from Platelet Lysate at the Surface of Electrospun Nanofibers for Tissue Engineering Applications

Dissertação de Mestrado
Mestrado Integrado em Engenharia Biomédica
Ramo Biomateriais, Reabilitação e Biomecânica

Trabalho efetuado sob orientação do
Professor Nuno João Meleiro Alves das Neves

outubro de 2013

DECLARAÇÃO

Nome: Ana Catarina Freitas Salazar de Oliveira

Endereço eletrónico: a55550@alunos.uminho.pt

Número do Bilhete de Identidade: 13728359

Título dissertação: Immobilization of Specific Growth Factors from Platelet Lysate at the Surface of Electrospun Nanofibers for Tissue Engineering Applications

Ano de conclusão: 2013

Orientador: Professor Doutor Nuno M. Neves

Designação do Mestrado: Mestrado Integrado em Engenharia Biomédica
Ramo: Biomateriais, Reabilitação e Biomecânica

Braga, _____/_____/_____

Assinatura: _____

Acknowledgments

This thesis is the last chapter of the five years I spent in University of Minho. And now is the time to acknowledge all the people, which in one way or another, guided and helped me during all this time.

First I would like to acknowledge my supervisor Professor Nuno Neves for all the help, support, knowledge and availability during this last six months. His enthusiasm about my project and all the ideas and suggestions were a great incitement during all the steps of this work.

I would like to thank Dr. Albino Martins for the supervision, help, suggestions, guidance and all the discussions about the project. Thank you for the patience and knowledge transmitted in areas and subjects I was less familiar. I also want to thank Dr. Ana Rita Pinto for the help during this project especially the time spent with the cell culture experiments. Thank you for your tips, supervision and suggestions.

I would like to thank all the people from 3B's. I would like to specially thank Nelson Monteiro for the first steps with the electrospinning and PCL meshes and his availability in helping me during my first months in the group. Diana Ribeiro, thank you for your help and always being available for my questions and the endless hours doing all those ELISAs. I would like to thank Dr. Margarida Martins, for the hints about statistical analysis.

I would like to thank the Maxbone and Osteography projects and also QREN for financing this reseach work.

Despite not being part of this thesis I would like to thank Professor João Mano for encouraging us to do ERAMUS, it was a fantastic experience that I would never forget. I would also like to thank Professor Marcel Karperien and Professor Aart van Apeldoorn for welcoming me in the DBE group in Twente. Thank you, Giulia, for helping me trough my first real experience in a lab as well as for introducing me into the cell culture world. All I learned there helped me during all the stages of this thesis. I would also like to thank all the friends I met there, it felt like home.

Thank you to the friends I made during this last five years, for always being there for me and all the moments we spent together.

To my friends from Biomedical Engineering ("Nata da Gata"). I could have not been here if it was not for the people that began this journey with me and that now are the friends that I will never get out of my sight again, we are a real family, that I am proud to be part of. It is amazing to see how we got here, how much we grow and how much our friendship is stronger as time goes by. We could write a book about all the stories and moments we shared together. But I know that much more chapters are about to come, we have a whole life ahead us. All the moments we shared together made me who I am today. Thank you all!

To all the people I had the opportunity to meet during my time in Academic Students Union. I am really proud for all the things we accomplished and done together. It was an amazing experience and the worst part was to say goodbye. When it hurts we know that it was completely worth it. I would like to give a special thank to Luís, Mateus, Pinheiro, Remi, Cléber, André, Ana Rita e Tita. It is really nice to see that the time we spent together turned into an incredible friendship.

To all my friends from Taipas. I know that in the last five years we didn't spend as much time as I would like together, but I have you always in my mind. Most of you are a part of my life since a long time and it is going to be like that for much more.

Tina, you know how important you are to me, you are my sister and sisters are meant for a lifetime. Since the first day at University we never got separated again. We are always there for each other. For 3ºA, for ERAMUS, for this five years, for the endless talks, for the help, for all the moments, for the wise advices, for the laughs, for all our crazy ideas that no one else would understand, for the future, for our moments, for your unconditional friendship, thank you! I could never have done this without you.

To André, for his patience, support and understanding. Thank you for everything.

To all my family: my grandparents, my uncles, my aunts and my cousins. Thank you for helping me whenever I needed, for being my friends and for believing in me.

To my brother and to my parents. Thank you so much for believing in me unconditionally, for all the support in every step I make, for encouraging me in pursuing my dreams. For always encouraging my work and for giving me all the opportunities. For picking me up whenever I felt down. I could have not done this without you, you are my model and my inspiration. I would never be able to thank you enough.

Abstract

One of the major problems related with implantable biomaterials is the limited bioactivity and suboptimal integration with the host tissue. The functionalization of biomaterial substrates to insert biological cues by the immobilization of biomolecules at their surface has been proposed as effective to overcome some of these limitations. Different immobilization strategies can be followed (such as adsorption or covalent immobilization) however, a critical aspect to have in consideration is to keep the bioactivity of molecule functionality. Therefore, the work developed in this thesis aims to activate and functionalize the surface of electrospun polycaprolactone (PCL) nanofiber meshes by the insertion of chemical groups (i.e. amine groups) to achieve a covalent immobilization of antibodies. The immobilization of the defined antibodies will allow for the selective binding of growth factors (GFs), either recombinant or derived from a biological fluid such as Platelet Lysates (PLs) that are known to have high concentrations of autologous GFs.

We determined the maximum immobilization capacity of the defined antibodies (i.e. TGF-β1, bFGF and VEGF) in the mentioned nanofibrous surface. The GFs of interest were further incubated into the corresponding biofunctionalized substrate, assessing the maximum binding capacity as well as the selective binding of the GFs from a pool of different proteins present in human platelet lysate samples. The bioactivity of the bound VEGF was further assessed by seeding and culturing a specific endothelial cell line (HPMEC-ST1.6R) over the biofunctionalized substrate. The biological data demonstrates that the immobilization strategy does not compromise the availability of the antibody neither the functionality of the bounded-GF. The combination of two antibodies (i.e. bFGF and VEGF) was tested in a mixed experiment or in separate regions of the same mesh in a side-by-side configuration. For the mix design, the biofunctionalized nanofibrous substrate was able to selectively bind two different GFs from the studied biological fluid. For the side-by-side a watertight chamber was developed to physically separate the substrate into two different areas, each one with a defined antibody just to validate the concept.

Our results confirm the efficiency of the immobilization method as well as the bioactivity of the bound GFs, showing a promising potential for the immobilization of different antibodies and corresponding GFs depending on the intended application. This strategy will enable designing advanced autologous therapies since both GFs and cells could be from the same donor, allowing the implementation of very effective and personalized therapies.

Resumo

Um dos grandes problemas relacionados com a implantação de biomateriais é a limitada bioatividade e integração com o tecido local. A funcionalização de substratos de forma a inserir sinais biológicos através da imobilização de biomoléculas na sua superfície pode ser uma tentativa para ultrapassar estas limitações. Diferentes técnicas de imobilização podem ser realizadas (por exemplo, absorção e imobilização covalente); contudo, um fator importante a ter em consideração é manter a bioatividade da molécula. Nesse sentido, o trabalho desenvolvido nesta tese tem como objetivo a ativação e funcionalização da superfície de nano fibras produzidas por electrospinning através da inserção de grupos amina de modo a conseguir uma imobilização covalente dos anticorpos. A imobilização de anticorpos específicos permitirá uma ligação seletiva de fatores de crescimento (FC), que podem ser recombinantes, ou retirados a partir de um fluído biológico, neste caso o Lisado de Plaquetas, que é conhecido por apresentar grandes concentrações de fatores de crescimento.

Ao longo deste projeto, diferentes ensaios foram realizados para determinar a capacidade máxima de imobilização de anticorpos (TGF-β1, bFGF e VEGF) no substrato acima mencionado. Os fatores de crescimento referidos foram então incubados no substrato nanofibroso correspondente, determinando a máxima capacidade de ligação, assim como a ligação específica dos fatores de crescimento a partir das diferentes proteínas presentes no lisado de plaquetas. A bioatividade do VEGF previamente ligado ao anticorpo foi determinada através de uma linha celular endotelial (HPMEC-ST1.6R). Os dados biológicos confirmaram que a estratégia de imobilização adotada não afetou a disponibilidade e funcionalidade do fator de crescimento. A combinação de dois anticorpos (bFGF e VEGF) foi testada misturando-os numa só solução ou então imobilizando-os lado a lado em áreas específicas da malha. No primeiro caso, através da mistura e consequente imobilização dos dois anticorpos, foi possível ao substrato biofuncionalizado selecionar dois fatores de crescimento distintos do Lisado de Plaquetas. Para a imobilização dos fatores lado a lado foi desenvolvido um sistema capaz de separar o substrato em duas áreas distintas, assegurando que as duas soluções não se misturavam.

Estes resultados confirmaram a eficiência do método de imobilização, assim como a bioatividade dos FC. Com esta estratégia será possível selecionar diferentes fatores de crescimento tendo em vista a aplicação pretendida, bem como a implementação de uma terapia autóloga possibilitando o desenvolvimento de tratamentos mais efetivos e personalizados.

Table of Contents

List of abbreviations

A

Ab – antibody

B

BMP – Bone Morphogenetic Protein

BSA – Bovine Serum Albumin

C

cm – centimeter

D

3D - Three dimensional

DNA - Deoxyribonucleic acid

DMF - Dimethylformamide

E

EGF – Epidermal Growth Factor

ECM – Extra Cellular Matrix

EDC - 1-Ethyl-3-(3-dimethylaminopropyl)carbodiimide

ECGS – Endothelial cell growth supplement

F

bFGF – Basic Fibroblast Growth Factor

FBS – Fetal Bovine Serum

G

GFs – Growth Factors

H

h – hour

HMD – Hexanediamine

I

IGF – Insulin Growth Factor

M

M – Molar

mM - Milimolar

mm – millimeter

µl – microliter

µm – micrometer

min – minutes

mL – mililiter

MTS – 3-(4,5-dimethylthiazol-2-yl)-5-(3-carboxymethoxyphenyl)- 2-(4-sulfophenyl)-2H-tetrazolium

MES – 2-(N-Morpholino)ethanesulfonic acid

N

NFMs- Nanofiber Meshes

NHS - hydroxysuccinimide

nm – nanometer

P

PCL- Polycaprolactone

PBS - Phosphate buffered saline solution

PL – Platelet Lysate

PRP – Platelet Rich Plasma

PEG – Poly (ethylene glycol)

PLGA – Poly (lactic-co-glycolic acid)

PLLA – Poly (L-Lactic Acid)

R

RT – Room Temperature

RM – Regenerative Medicine

S

SEM – Scanning Electron Microscope

T

TGF-β1 – Transforming Growth Factor

TE- Tissue Engineering

U

UV- UltraViolet

V

VEGF – Vascular Endothelial Growth Factor

v/v – Volume/volume

W

wt/v – Weight/volume

List of Figures

Chapter 1 – Introduction

Chapter 2 – Materials and Methods

Chapter 3

supplemented medium (ECGS) ; NFM with immobilized VEGF antibody (NFM_Ab2), NFM with bound recombinant VEGF (NFM+$VEGF_{Rec}$) PL-derived VEGF (NFM+$VEGF_{PL}$) with non supplemented media a) Cell Proliferation, b) cell viability, c) total protein synthesis and d) intracellular VEGF synthesis. Statistical analysis was performed for the five different conditions comparing each time point (Day 1, Day 3 and day 7). Data was considered statistical different for p values < 0.05. (*****) denote significant differences when compared to NFM condition, (+) when compared to NFM_Ab1 supplemented media, (x) when compared to NFM_Ab2, (#) when compared to NFM_VEGF and (&) when compared to NFM_PL.

Figure 3.8 (a) Quantification of mixed immobilized bFGF and VEGF antibodies. (b) Relative quantification of bound GFs (i.e. VEGF and bFGF) derived from PL.

Figure 3.9 Spatial distribution of the mixed immobilized primary antibodies at the surface of a single activated and functionalized Nanofibrous substrates. The bFGF and VEGF antibodies were simultaneously immobilized in the same mesh, at the previously optimized concentrations. a) Alexa Fluor ® 448 was used as the secondary antibody for the anti-bFGF); b) the Alexa Fluor ® 594 was used for the anti-VEGF; c) the spatial distribution of the two primary antibodies (merge view); and d) activated and functionalized Nanofibrous substrates without primary antibodies immobilization.

Figure 3.10 Laser scanning confocal microcopy image demonstrating the side-by-side antibodies immobilization over the same activated and functionalized Nanofibrous substrate.

List of Tables

Chapter 1

Chapter 3

Chapter 1 Introduction

Chapter 1

Introduction

Growth factors immobilization for tissue engineering and regenerative medicine therapies

1.1 Abstract

To achieve a more effective and faster regeneration of tissues and organs, the immobilization of bioactive molecules at the surface of biomaterial substrates has attracted tremendous interest as a promising Tissue Engineering and Regenerative Medicine approach. Growth factors as bioactive molecules play a pivotal role in wound healing cascade and have a significant role in a wide range of cellular events, such as proliferation, migration, cell signaling and differentiation. There are different immobilization strategies that can be followed to functionalize the biomaterial substrates with growth factors. However, a critical issue is the preservation of the bioactive molecule functionality after immobilization. Covalent immobilization is able to accomplish those requirements, leading to the development of devices with high functionality and to successfully achieve localized and sustained growth factor availability. Biological samples, like platelet rich plasma (PRP), have gained special interest mainly due to the easy assessability, variety and autologous source of growth factors envisioning personalized therapies. In this introduction we will discuss the various growth factors immobilization strategies available and its applications.

Key Words: Growth Factors, Immobilization, Biomaterials, Platelet Rich Plasma, Regenerative Medicine, Tissue Engineering

1.2 Tissue Engineering and Regenerative Medicine

Injuries and diseases can affect tissues and organs which may result in the partial or total loss of function. When no medical intervention is conducted, the physiological response of the body is restricted and is mostly confined to the auto-regenerative process. This might be an effective response to small injuries, but does not lead to the restoration of the normal structure and function of large defects [1–3]. In the last decades, the conventional treatment modalities relies on the replacement of the affected organ or tissue by synthetic implantable devices that can restore the tissues' or organs' function [1,4]. Current clinical therapies for restoring tissue structure and function largely rely on the: transplantation of organs (such as kidney, liver, heart, lung, pancreas); on the use of tissue transplants (such as autografts, allografts or xenografts), on the administration of growth factors (GFs) and on the implantation of artificial devices (metal-alloys, ceramics or other prosthesis) [1,5]. Regrettably, these strategies not always have the desired outcomes mostly caused by immune rejection, insufficient biocompatibility, the required mechanical and physical properties, complicated surgical procedures, chronic inflammation and lack of clinical predictability. With artificial implantable devices, the patient needs to face problems often related with the reliability and the fitting of the device into the defect site.

Due to the increased incidence of injuries and diseases, and the medical need to create more effective therapies for improving the outcome of current types of tissue loss, the field of Tissue Engineering and Regenerative Medicine (TERM) has proposed alternative solutions and strategies that can overcome some of those limitations [3,6]. The increasing knowledge on wound healing and tissue formation physiology, as well as the advances made in materials science and cell biology, is essential to the development of effective strategies [1,3]. The TERM research aims at replicate these physiological processes, in order to develop more efficient hybrid systems for a complete restoration of damaged organ or tissue [1,7–9].

Tissue Engineering (TE) aims to create, replace and facilitate the regeneration of damaged or diseased tissue with the combination of three different fundamental factors: biomaterials (scaffolds), cells and bioactive molecules (in most cases GFs) (**Figure 1.1**). The final purpose of TE is to create a tissue construct that upon transplantation will give raise to similar tissue found in the body.

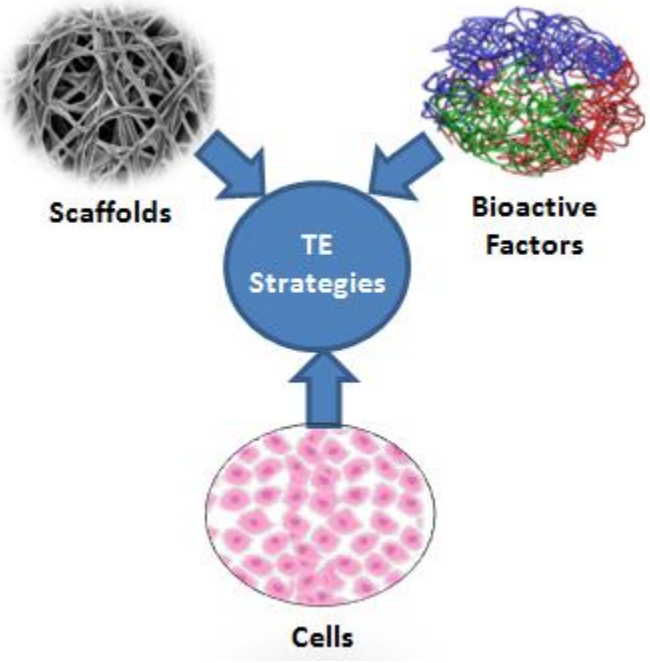

Figure 1.1 The three fundamental components of a Tissue Engineering strategy: a) biomaterial scaffold; b) relevant cell communities and c) bioactive molecules.

TE approaches that may be followed are: (a) the delivery of tissue-inducing molecules that stimulate host cells to function normally; and (b) the development of a 3D matrix or scaffold biomaterial in which cells grow to create a living 3D tissue substitute [7–9]. The former strategy is the most commonly followed in the field of TE, where living cells are seeded in a natural and/or synthetic substrate in order to create implantable devices able to restore the function of tissues. In this strategy, the required bioactive molecules (such as GFs, cytokines and proteins) are often supplied in the culture medium or may be released by drug delivery system [7,9,10].

1.2.2 Requirements of a biomaterial scaffold

The scaffold plays a unique role in the TE strategies since it is designed to serve as a temporary support for the cell proliferation, migration and differentiation, in order to form a hybrid tissue construct *in vitro* [4]. During the past two decades, many studies have been conducted in the development of biomaterials scaffold with potential applicability in clinical TE strategies. For that reason, scaffolds should have the following properties: (a) promote cell-biomaterial and cell-cell interactions, cell adhesion and ECM deposition [7,11,12]; (b) facilitate a sufficient transport of gases, nutrients and other soluble factors, to allow cell survival,

proliferation and differentiation [7,13]; (c) biodegradability in a rate compatible to the kinetics of tissue growth [14]; (d) act as delivery vehicles for biomolecules and bioactive factors [13]; (e) support the stress developed at the implant site and retain mechanical strength after implantation, [15]; (f) the porosity and the pore size should allow the cell ingrowth, an uniform cell distribution and migration, an improved ECM deposition and facilitate neovascularization of the construct [7,16,17]; (g) provoke a minimal degree of inflammation or toxicity *in vivo* [18].

1.2.2 Cell sources

The cell is the basic structural and functional unit of a living organism. Multicellular organisms are made up of many different cell types with specialized functions [19]. These specialized cells enable performing specific functions. Depending on the final application and the tissue to be repaired, different cell sources can be selected and expanded *in vitro* such as the hematopoietic, endothelial, chondrocytes, osteoblasts, epithelial cells [20].

When cells are used for TE approaches, a biopsy of a donor tissue is dissociated into individual cells. Indeed cells source can be xenogenic (such as bovine or porcine), allogenic (donor from the same species but from a different individual) or autologous (from the patient itself). The preferred cell source to use in a TE strategy is the autologous cells, where a biopsy of a donor tissue is obtained, followed by the cells dissociation and expansion *in vitro*, and, finally, their implantation into the host [10]. One of the limitations of applying cell-based regenerative medicine therapies to organ replacement is the difficulty of obtaining sufficient number of cells in relevant therapeutically quantity, as well as the protocols of *in vitro* cell manipulation are not completely elucidated [21].

While several tissues remain important cell sources of therapeutic relevant differentiated cells, stem cells have emerged as a very strong alternative. Stem cells have the remarkable potential to differentiate into different cell types in the body. They serve as an endogenous repair system, able to participate in the permanent homeostasis and maintenance of the organs dying cells. Stem cells are distinguished from other cell types by two important characteristics: they are unspecialized cells capable of renewing themselves through cell division (the self-renewal capacity) and they can give rise to specialized cell types under certain physiologic or experimental conditions (the differentiation capacity) [22–24]. Therefore,

when a stem cell divides, each new cell has the potential either to remain as a stem cell or to become another cell type with a more specialized and differentiated function.

Stem cells can be characterized as totipotent (ability to differentiate into the cells of all the tissues of an entire organism) pluripotent (the potential to differentiate into most specialized cells in the body, but not all the tissues of an organism) and multipotent (the ability to form multiple cell types). [23] There are different types of stem cells: the embryonic stem cells (ESCs) [25], responsible for embryonic and fetal development and growth; the adult stem cells (ASCs)[26], responsible for the growth, tissue maintenance, regeneration and repair of diseased or damaged tissue.

1.2.3 Bioactive molecules: growth factors

Different signals from the extracellular microenvironment can play significant roles over the cellular performance, namely insoluble extracellular matrix (ECM) macromolecules, diffusible/soluble molecules, and cell–cell receptors **(Figure 1.2 a)**. Although the growth factors (GFs) belong to the category of soluble molecules, they can also be present in the immobilized form within the ECM. The diffusible/soluble molecules (including the GFs) can have different ways of action over cellular activity: autocrine (cell secretes molecules that binds to receptors on that same cell, leading to changes in that same cell), paracrine (cell produces a signal to induce changes in nearby cells) and/or endocrine (communicate a molecule over a long distance; the signals are released from a cell, migrate with the bloodstream and can travel around the entire body) **(Figure 1.2 b)**. Growth factors bind to specific receptors on target cells and regulate the gene expression controlling functions such as cell growth, tissue morphogenesis, wound healing and regeneration [6,27].

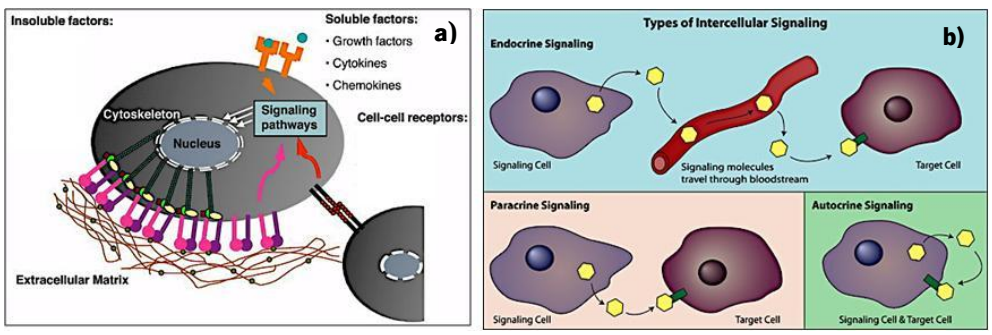

Figure 1.2 The extracellular microenvironment (a) and cell signaling trough soluble factors. Adapted from [28]

The bioactive signals (like proteins, GFs, cytokines) involved in tissue repair or function restoration also can play a fundamental role in TERM strategies. A precise control over the levels and sequence of the signaling molecules within a specific location may positively regulate the regenerative processes [9,27]. Proteins, especially GFs, have an important role in the regulation of a variety of cellular processes, namely in the growth, migration, differentiation and apoptosis of specific cells. Additionally, the activity of GFs is particularly connected when an injury occurs, by coordinating the healing process, until the wound is completely repaired [6,27]. Another important aspect related to the function of GFs is there crucial role in the exchange of information between different cell populations and their microenvironment (paracrine effect) [6,29,30].

1.2.3.1 Growth factors and the healing cascade

GFs are known to play a pivotal role in the complex cascade of the physiological repair mechanism by providing the needed signals to the cells and, thereby, leading to an accelerated functional restoration of damaged or defective tissue [31]. Wound healing is a complex biological process that involves inflammation, mitosis, angiogenesis, synthesis of proteins and ECM remodeling [32]. There are different GFs with different specific targets and functions that are involved in all the phases of the healing process: Vascular Endothelial Growth Factor (VEGF), Basic Fibroblast Growth Factor (bFGF), Epidermal Growth Factor (EGF), Insulin Growth Factor (IGF), or Platelet derived growth factor (PDGF) [29,31,33].

In a simple way, the healing cascade involves three different phases: inflammation, a trophic phase (including angiogenesis, proliferation and synthesis of ECM) and remodeling. When a tissue is damaged or injured, the healing cascade begins immediately when platelets come into contact with collagen. After platelet activation, clothing factors, cytokines and growth factors are released initiating the healing response [31,34].

The inflammatory response is characterized by leucocyte extravasion and accumulation at the injury site, and monocyte/macrophage activation [35,36]. PDGF initiates the chemotaxis of neutrophiles, macrophages, smooth muscle cells and fibroblast. TGF-β is another important signal for the initiation of the healing cascade by attracting macrophages, stimulating them to produce additional cytokines like FGF that enhances collagen synthesis. TGF-β further enhances collagen expression leading to a strong response of the matrix

producing cells to ensure a rapid deposition of new connective tissue at the injury site and developing the fibrous cloth [37,38].

The trophic phase includes the activation of endothelial cells to initiate the angiogenic process, which is the formation of new blood vessels able to promote blood flow, to support the high metabolic activity of the new tissue (avascular tissue are not comprise in this angiogenic phase)[39]. VEGF stimulates this process provinding a new blood supply to the injured site. As the healing process progresses, several other important responses are activated. The cells migrate into the injury site, using the fibrin matrix as a scaffold, then divide and differentiate, producing collagen, proteoglycans and other components of the natural ECM [31]. Finally, during the remodeling stage, there is a decrease in cell density and, therefore, on the metabolic activity of the injured tissue. As stated above all these processes are mediated and activated by signaling molecules, like GFs, that limit the duration of each phase and promote the progression into the next stage [31,40,41].

The basis of TERM research relies on the engineering of a microenvironment able to mimic the critical aspects of the natural healing process, namely the wound healing cascade, by providing suitable biochemical and physical factors.[6] However, due the high complexity of this process these biological systems are not easy to recreate *in vitro* [6].

Therefore it is absolutely necessary to provide the cells with a local biochemical and mechanical niche that can mimic the natural environment in which they can proliferate and differentiate efficiently, by creating an artificial ECM and by delivering GFs. In order to induce the regeneration and to accelerate the capability of tissue growth, it is fundamental to create an environment that can mimic the natural wound healing cascade. Due to all these aspects, the integration of GFs and the development of biomaterials that mimic the ECM microenvironment play an important role in the cellular regulation of adhesion, proliferation, differentiation and gene expression.

1.2.3.2 Growth factors: properties and roles

GFs have different mechanisms of action depending on the concentration, on the half-life time, on the phenotype of the target cells as well as on their presentation (soluble or immobilized in the ECM) [6,30,42]. The local and systemic administration of GFs are therapeutic alternatives used in the treatment of chronic wounds (like ulcers, post-surgical wounds) as

well as the repair and regeneration of tissues in different fields like plastic surgery, orthopedics and cartilage lesions, muscle injuries and skin [29,30]. The different GFs used in therapeutic applications are presented in **Table 1**.

To be effective as a therapeutic agent, a GF has to reach the target site without suffering biological degradation and, it has to remain at the target location sufficient time to exert its actions. GFs that are provided exogenously in solution at the site of the injury tend to be not effective because they tend to diffuse away from the wound site, being susceptible to enzymatic digestion or inactivation [6]. In summary, various aspects have a significant effect on the therapeutic efficacy of GFs, including their short half-life *in vivo*, the side-effects caused by the administration of multiple or high doses of GFs to reach the desired effect at the target cells, and the possible denaturation of the GFs during manipulation and circulation. All these issues should be taken into account when designing a successful GF-based therapy [6,43,44].

When designing an implantable system, some specific requirements related to the GFs should be of prior interest: the type of GF to be used and its final application; a feasible preparation method that does not affect the GF bioactivity; a robust system that can restrict the protein conformational mobility and protect the protein from physical and chemical degradation; a high loading efficiency; the ability of the system to retain the GFs at the site of action; a presentation of the GFs that mimics the temporal profile of the healing process *in vivo* [6,45,46].

Table 1 Most commonly used Growth Factors: biological role and targets

GF	ROLES	TARGETS	REFERENCES
TGF-β1	Promotes the production of extracellular matrix; Modulates and enhances the proliferation of fibroblasts; Increases and stimulates synthesis of collagen type I; Enhances the proliferation of bone cells.	Bone/ Cartilage	47–50
FGF	Potent inductor of cell proliferation; Promotes angiogenesis and differentiation; Collagen production.	Bone/ Cartilage/ Periodontal tissue	51–53
PDGF	Stimulates fibroblast production, angiogenesis and macrophage activation; Collagen synthesis.	Cartilage/ Bone/ Angiogenesis	54,55
EGF	Triggers the expression of genes that leads to DNA synthesis and proliferation; Promotes mesenchymal and epithelial cell differentiation, angiogenesis and proliferation.	Skin/ Cornea/ Nervous System	56–58
IGF	Chemotactic for fibroblast and stimulates protein synthesis; Enhances bone formation by the proliferation and differentiation of osteoblasts.	Bone/ Dermal wound healing/ Pancreatic stem cell differentiation	59–63
VEGF	Promoter of angiogenesis and vasculogenesis; Proliferation of endothelial cells; Increases microvascular permeability.	Vascularization/ Stem cell differentiation	64–66

1.3 Growth factors sources

Peripheral blood is constituted by different cellular elements like red blood cells, white blood cells and platelets. These components are found in the peripheral circulating blood and are not retained and sequestered by the lymphatic system, spleen, and liver**.** Certain medical conditions in which the patients lose some of the blood components may require a blood transfusion. Nowadays, there is no need to make a transfusion of the whole

blood, being possible to select only the components of interest (like platelets, plasma, clothing factors) [67,68].

In the past decades, platelet rich plasma (PRP) has been increasingly used in many medical fields, with particular interest in orthopedics and musculoskeletal disorders in athletes that need a fast recovery and early return to competition [31,69,70]. PRP is described as "a fraction of autologous plasma containing an above baseline platelet concentration and growth factors which take part in the post-traumatic healing process"[71]. Therefore, to be defined as PRP, the platelet count should be at least 1 000 000 platelets/µl, whereas a platelet normal count ranges from 150 000 to 350 000 platelets/µl. Since platelets are a source of GFs, there is a growing interest in the use of PRP as a strategy to optimize the healing of the tissues [72].

The impact of the discoveries regarding the potential of PRP healing has increased the optimism about autologous based regenerative medicine. PRP is also a cost-effective product, since it is taken from a simple blood samples and, therefore, it is easy to implement this cost-effective source in the current clinical practice. The **Figure 1.3** depicts the simplicity of the PRP preparation procedure. Additionally, since PRP is a concentrated extract of lysed platelets, it is also a source of fundamental growth factors that are secreted by the platelets when a wound healing process is initiated. Because it is an autologous source of GFs, less regulatory concerns exist about its biosafety, since the immunogenic reaction and the possibility of disease transmission are eliminated. However, due to its complex composition of proteins, growth factors and cytokines, the mechanisms of action and dosage still need to be elucidated[41,73].

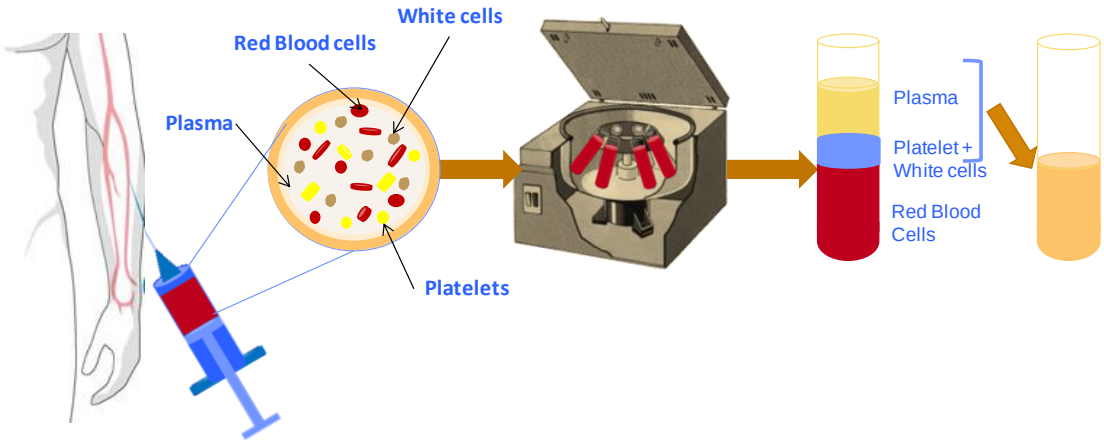

Figure 1.3 Schematic representation of the PRP process. In this procedure about 30 to 60 ml of blood is taken from the donor and centrifuged during 15 minutes and 3200 rpm. With this centrifugation step it is possible to separate the different constituents of the human blood. PRP can be storage until further use and upon activation PRP facilitates the local release of different GFs for tissue engineering therapies.

The possible use of PRP as an alternative biological source of bioactive agents has gained a special and exciting interest in TERM approaches [31,73]. The use of PRP aims to take advantage of autologous source of bioactive molecules, such as GFs, proteins and cytokines, envisioning an autologous therapy where it is possible to use patient specific therapies. Recent reports suggest that the use of PRP may be an approach to develop clinically relevant materials (GFs+scaffolds) able to deliver GFs and simultaneously to allow cell culture, and ultimately, integrate the *in vitro* generated construct into the native tissue environment [41,74–76]. However, there are some controversial works where it is reported that the use of PRP is not effective [70,77,78]. Since the use of PRP is still in an early stage, new preparation methods and applications need to be explored to maximize its efficiency in TERM strategies. It is also necessary to determine the optimum concentration of the various GFs present in the PRP, which result in more effective PRP-based treatments.

1.4 Immobilization methods and strategies

The GFs released in physiological environments are susceptible to inactivation by degradation, prior to the possibility of reaching the desired target cells. Therefore, high quantities of soluble GFs well above the physiological values may be needed to have the required effects at the cellular level. However, the delivery of high quantities of GFs may lead

to undesired cells and tissues side effects related with toxicity. Biomaterial-based systems can be designed to deliver soluble GFs locally, but sometimes they can be ineffective and costly [6,42,79]. To overcome some of these drawbacks on the use of GFs as therapeutic agents, the biofunctionalization of substrate surfaces by the immobilization of GFs has special interest mainly due to the need to optimize the biological performance of implantable medical devices [80].

An important requisite of protein immobilization is the biocompatibility and bioactivity of the substrate surface, because it should interact positively with the native structure of the proteins and biomolecules [81]. The substrate chemistry, particularly the availability of reactive groups, is an important factor to consider when selecting an appropriate immobilization strategy. The location of such reactive groups, relatively to the receptor-binding area of the GF structure, and the dimensions of the substrate are other important aspects to have in consideration. Furthermore, the immobilization of GFs generally requires the use of aqueous-based chemistry, as most of the GFs are either not soluble or may become denaturated in the presence of organic solvents [6,42,82–84].

This section will mostly be focused on the immobilization strategies that involve the direct binding of the GF to the surface of the biomaterial substrate. Different immobilization methods can be implemented to achieve the biofunctionalization of substrates such as adsorption, physical entrapment and covalent-immobilization [42,82]. However, each immobilization method results in advantages as well as in limitations. Covalent immobilization is the most reported method, which leads to a strong and stable binding of the bioactive molecule to the substrate. However, the presence of functional groups is required in both the substrate and the molecule to be immobilized. In most of the cases, a linker reagent is necessary. With this method it is also possible to overcome the common problems associated to the adsorption method, namely the deadsorption or the denaturation of the antibody [82,85].

1.4.1 Non-covalent immobilization

The immobilization of GFs can be divided in two different main categories: non-covalent and covalent immobilization. Non-covalent immobilization includes physical entrapment, adsorption or ionic complexation [83]. Physical entrapment is often associated with

GFs encapsulation/incorporation into micro-particles or reservoirs. Adsorption of GFs typically takes advantage of direct interactions, such as surface electric -charge or other secondary interactions between the GFs and the substrates surface, or of indirect interaction via intermediate proteins or other biological molecules [83,86,87]. A third approach of non-covalent immobilization of GFs to a biomaterial is ion complexation. Proteins with different isoelectric points may be used for polyion complexation with charged macromolecules. These methods tend to have some problems associated such as the desadsorption and the irreversible ion complexation that can cause protein inactivation and denaturation [9,83].

To improve the stability and persistence of the GFs immobilization, and consequent delivery to target cells and tissues, covalent immobilization of GFs to the substrate emerged as an alternative approach. Despite being a more complex process, immobilization strategies can prolong GFs availability than those obtained with weak physical immobilization. Also, the covalent immobilization allows a spatial control over the GF distribution and reduces the amount of GFs required, thereby potentially reducing the cost and increasing the efficacy of various bioactive materials or engineered tissues. Furthermore, the presentation of GF in an immobilized form also has physiological relevance, as both soluble and matrix-bound GFs perform distinct functions in the *in vivo* environment [6,42,88].

1.4.2 Covalent immobilization strategies

For the covalent immobilization of bioactive molecules, different chemical and reactive groups are needed in both the substrate and the GFs of interest. For different covalent immobilization methods, different groups are required. The most common reactive groups of GFs are the amines or the carboxyl groups [84]. Whereas in the substrate surfaces, besides the amines and the carboxyl groups, also double bonds, C-H, N-N and acrylates are frequently required[89]. If the substrates do not have the required chemical groups, chemical treatments can be performed to activate their surface.

Covalent immobilization often requires a linker to achieve a more stable and strong binding of the GF to the substrate. For example, 1-Ethyl-3-(3-dimethylaminopropyl) carbodiimide (EDC) couples the carboxyl groups to the amine groups, resulting in a stable amide bond. In this reaction, EDC reacts with carboxyl groups to form an o-acylisourea

intermediate, which further reacts with the amine-containing molecule. However, this intermediate is highly unstable in aqueous solution and susceptible to hydrolysis, which results in re-formation of the carboxylic acid. Thus, sulfo-N-hydroxysuccinimide (sulfo-NHS) or N-hydroxysuccinimide (NHS) may also be added to create a more stable amine-reactive sulfo-NHS or NHS ester intermediate, which increases the efficiency of the reaction. This coupling procedure is simple, inexpensive, effective and can be performed under mild conditions [42,90,91].

Other methods of GFs immobilization involve the use of a photo-initiated reaction, which allows the binding of the GFs to a substrate [92,93]. The first step of this method relies on the functionalization of the GF with a photo-reactive group and, afterwards, the binding of the modified GF to the substrate surface take place upon exposure to a defined radiation wavelength (usually, ultra-violet light) [94]. One significant advantage of the photo-immobilization method is the simple development of patterned GFs, which can be easily performed through the use of photomasks or by the precise irradiation of specific areas with laser light sources, leading to a spatial defined distribution of the immobilized GFs. The creation of immobilized GF patterns enables greater control over cell function. Like the GFs immobilization by the use of EDC, photo-immobilization is relatively simple and effective but the use of photomasks frequently involves expensive technologies. The use of crosslinking reagents or the photo-immobilization approaches also may have problems related with the GFs bioactivity, bioavailability and protein configuration. Specifically, the potential caused to the damage GFs by the ultra violet light is considered the most important drawback [42,82,94].

Functionalization of polymers with acrylate groups is a common method for the activation of biomaterials that can be further cross-linked upon exposure to UV. Crosslinked networks of acrylated polymers are formed via chain-growth polymerization of the acrylates, and this process is initiated by reactive centers, such as radicals, which are generated upon photo-cleavage of the initiator molecules. These free radicals propagate through the unsaturated vinyl bonds on the acrylated polymers, resulting in covalently crosslinked high molecular weight polyacrylate kinetic chains. However, the bioactivity and orientation of the immobilized GFs can be compromised. Because this immobilization strategy depends upon acrylate reaction with another acrylate, the types of substrates that can be used are generally restricted to acrylated polymers, such as PEG-DA [42,84,85].

By immobilizing GFs onto the surface of biomaterials, they are more protected against cellular inactivation and digestion. As a result, the immobilized GFs have more sustained and

longer activity when exposed to physiological environments. Growth factor immobilization may also overcome the diffusion limitations of soluble GFs. While the soluble delivery of GFs elicits responses in the surrounding environment, covalently immobilized GFs may have the additional advantage of inducing local effects within the scaffold where the cells are seeded, maximizing its effect. Maximum interaction with cells in the implant sites facilitates integration with the host tissues [6,27,88].

1.5 Applications of immobilized growth factors

The effect of soluble GFs over the behavior and signaling of different cell types has been widely described in the last years. However, in what concerns the influence of immobilized GFs, the available information is sparse and the outcomes much less reported. Soluble GFs are recognized by their corresponding cell-surface receptors and, thereafter, are internalized as a complex. In the case of immobilized GFs, cells are not able to internalize those receptor-GFs complexes, leading to a more sustained activation of the intracellular pathways. Consequently, with the immobilization of GFs it is possible to achieve enhanced and unique cellular responses that cannot be achieved with soluble GFs [27,95]. Due to the improved stability and spatial control offered by the immobilization of GFs, this approach may provide beneficial contributions for different tissue repair strategies. The next sections will focus on the most promising results on the application of immobilized GFs at the surface of substrates. The effects of immobilized GFs have been studied in various areas including angiogenesis, bone repair and regeneration, dermal wound healing, cartilage repair, pancreas and liver, nerves and stem cell differentiation.

1.5.1 Angiogenesis

One of the major problems associated with tissue engineered therapies is the lack of a functional and integrated vascular system. The flow of nutrients and oxygen and the cell metabolites are essential to maintain the viability and functionality of tissues. Particularly, an inadequate vascular system leads to mal-function in mass transport and gases exchange which may cause unwanted cellular necrosis [96,97].

Endothelial cells are the responsible for the capillary vascular network formation (angiogenesis). Almost all tissues depend on a blood supply, and the blood supply depends on endothelial cells, which form the linings of the blood vessels. Endothelial cells have a remarkable capacity to adjust their number and arrangement to suit local requirements [98].

The formation of new blood vessels can occur during different events, such as wound healing, organ regeneration, and in the formation of the placenta, as well as in several pathological processes (e.g. tumor growth, rheumatoid arthritis, diabetic retinopathy). A switch to the angiogenic phenotype depends on a local change in the balance between angiogenic stimulators and inhibitors. Furthermore, angiogenesis process is regulated by a complex control system, mediated by soluble molecules, such as VEGF [99]. In the *in vivo* physiological environment, both matrix-bound and soluble forms of VEGF can be found. Soluble VEGF is believed to induce endothelial cell proliferation, whereas matrix-bound VEGF tends to promote the vascular sprouting and branching associated to neovasculature. Immobilized VEGF has been found to successfully stimulate the proliferation of endothelial cells [65,99].

Due to the short half-life and the transient effect of soluble VEGF the development of strategies to achieve a more controlled delivery and release of this GF is of utmost importance. Accordingly, the immobilization of VEGF has become a promising strategy to overcome these problems, as a more suitable system to have control over the angiogenic process and endothelial cell function. With this strategy a microvasculature system would be incorporated in some engineered biomaterial substrates and scaffolds leading to more efficient tissue engineered solutions [42,100]. Recent reports demonstrated that the covalent immobilization of VEGF on different substrates and scaffolds improved the endothelial cells tubulogenesis as well as stimulates their proliferation [101,102]. The release of soluble VEGF sometimes results in vessels that are not completely functional. For that reason, VEGF was also co-immobilized with other GFs in other to achieve a more efficient and functional angiogenic process. Angiopoetin-1 (a GF related to the vessels stability and maturation) was co-immobilized with VEGF and the biological results demonstrated a significant improved tubulogenesis, as well as endothelial cell infiltration [103,104]. Another example of GF involved in the angiogenesis process, PDGF-ββ was also immobilized to improve the formation of a functional engineered microvasculature [105]. Despite significant efforts and promising results in developing a functional vascularization system by the immobilization of more than one GF to

improve angiogenic and vessel stability, those strategies still need further demonstration of efficacy.

1.5.2 Other relevant applications: dermal healing, cartilage, bone and stem cells differentiation

The use of GFs has been explored in different tissues, namely in the healing of chronic dermal wounds, overcoming the problems often associated with pain, long-term recovery, high cost and unsuccessful treatment outcome. With the GFs immobilization approach, a more controlled bioavailability of the GFs is possible, overcoming the problems of inadequate delivery of soluble GFs. Also of note is the prolonging bioactivity and half-life of the GFs. EGF immobilization was reported in most studies of dermal wound healing, since it stimulates the migration and proliferation of dermal cells (example: fibroblasts) that play an important role in wound closure. It was demonstrated that lower amounts of immobilized EGF are needed, when compared to the soluble EGF, to have a positive effect over the cellular response [42,106–108].

Embryonic and adult stem cells have the capacity for self-renewal and also have the ability to differentiate into different cell types. Stem cell differentiation can be achieved in vitro by the application of different molecules and signals. Recent studies evaluated the response of stem cells to immobilized GFs. A wide range of final applications was explored including the immobilization of GFs to promote neural differentiation (PDGF-AA and IFN-ϒ) and VEGF immobilized to differentiate the stem cells into vascular or hematopoietic cell types [109–112].

Recent efforts have focused on helping the body to restore cartilage, through cell-based and/or biomolecules therapies. A variety of synthetic- and natural-origin polymers were proposed for this purpose, each of it with their benefits and drawbacks. To date, an ideal biomaterial has yet to be created that can promote the functional repair or regenerate the damaged cartilage [113]. However, the addition of signaling molecules such as the GFs seems to be a promising control to facilitate cartilage regeneration therapies.

TGF-beta was proposed to stimulate chondrogenesis through intracellular pathways [114]. TGF-β3 was immobilized into different scaffolds to solve and treat some cartilage injuries and lesions. Also TGF-β1 was immobilized at the surface of different polymers. In both cases the expression of chondrogenic gene markers was significantly increased, as well as the production of glycosaminoglycans and collagen type II, indicating that neo-cartilage was generated.

The gold standard treatment of bone fractures and other orthopedic injuries causing loss of bone tissue rely on the use of autologous bone grafts. However, despite their biocompatibility and exceptional osteoconductive properties, autografts are associated with donor site morbidity. The most widely used ostegenic inducing molecules are the BMPs (namely the BMP-2 and the BMP-7, already approved by the FDA for human use) that induce new bone formation and regeneration at specific sites (used for example in orthopedic applications such as spinal fusions and oral surgery) [115–117]. In these products, BMPs are delivered to the site of the fracture by being incorporated into a bone implant, and released gradually to promote bone formation. However, the delivery method of BMPs often shows a lack of local retention and the need of high amounts of proteins to achieve the desired biological effects. The immobilization of such GFs may have favorable outcomes in bone tissue engineering strategies, as well as on the osteointegration of orthopedic implants, with the use of significantly lower amounts of GF to achieve effective osteogenic outcomes [42]. BMPs were immobilized in different substrates such as PLGA scaffolds [118], chitosan membranes [119] and PCL scaffolds [120] showing that the biological effect of immobilized BMP-2 can significantly increase the expression of osteoblastic differentiation markers, when osteogenic precursor cells are cultured. When comparing the *in vivo* efficiency of the soluble BMP-2 and the immobilized form, the immobilized approach showed that both the amount of bone and its maturity have increased [42,118–120].

1.6 Final Remarks

The implementation of chemical immobilization strategies allows the development of highly effective GF delivery systems, promoting the direct interactions between the immobilized GFs and the resident cells and avoiding the potential side effects caused by systemic administration. The biggest challenge of this strategy relies on finding the correct balance between the GFs and the physicochemical properties of the scaffold that can regulate cell behaviors in designing highly effective strategies. By combining biomaterial scaffolds with immobilized GFs at the surface were cells are seeded it will be possible to have a strongest interaction with the host tissues

1.7 References

1. Williams, D. F. To engineer is to create: the link between engineering and regeneration. *Trends Biotechnol.* 24, 4–8 (2006).
2. Langer, R. & Vacanti, J. P. Tissue engineering. *Science* 260, 920–6 (1993).
3. Fuchs, J. R., Nasseri, B. A. & Vacanti, J. P. Tissue engineering: a 21st century solution to surgical reconstruction. *Ann. Thorac. Surg.* 72, 577–91 (2001).
4. Saltzman, W. M. *Tissue Engineering: Engineering Principles for the Design of Replacement Organs and Tissues*. 544 (Oxford University Press, USA, 2004)
5. Yarlagadda, P. K. D. V, Chandrasekharan, M. & Shyan, J. Y. M. Recent advances and current developments in tissue scaffolding. *Biomed. Mater. Eng.* 15, 159–77 (2005).
6. Chen, F.-M., Zhang, M. & Wu, Z.-F. Toward delivery of multiple growth factors in tissue engineering. *Biomaterials* 31, 6279–308 (2010).
7. Dhandayuthapani, B., Yoshida, Y., Maekawa, T. & Kumar, D. S. Polymeric Scaffolds in Tissue Engineering Application: A Review. *Int. J. Polym. Sci.* 2011, 1–19 (2011).
8. Atala, A. Tissue engineering and regenerative medicine: concepts for clinical application. *Rejuvenation Res.* 7, 15–31 (2004).
9. Lee, K., Silva, E. A. & Mooney, D. J. Growth factor delivery-based tissue engineering : general approaches and a review of recent developments Growth factor delivery-based tissue engineering : general approaches and a review of recent developments. (2011). doi:10.1098/rsif.2010.0223
10. Atala, A. Engineering tissues , organs and cells. 83–96 (2007). doi:10.1002/term
11. Boyan, B. D., Hummert, T. W., Dean, D. D. & Schwartz, Z. Role of material surfaces in regulating bone and cartilage cell response. *Biomaterials* 17, 137–46 (1996).
12. Moroni, L. & Elisseeff, J. H. Biomaterials engineered for integration. *Mater. Today* 11, 44–51 (2008).
13. Garg, T., Singh, O., Arora, S. & Murthy, R. Scaffold: a novel carrier for cell and drug delivery. *Crit. Rev. Ther. Drug Carrier Syst.* 29, 1–63 (2012).
14. Hutmacher, D. W. Scaffolds in tissue engineering bone and cartilage. *Biomaterials* 21, 2529–43 (2000).
15. Meyer, U.; Meyer, Th.; Handschel, J.; Wiesmann, H. P. *Fundamentals of Tissue Engineering and Regenerative Medicine*. (2009).
16. Puppi, D., Chiellini, F., Piras, a. M. & Chiellini, E. Polymeric materials for bone and cartilage repair. *Prog. Polym. Sci.* 35, 403–440 (2010).
17. Leong, K. F., Cheah, C. M. & Chua, C. K. Solid freeform fabrication of three-dimensional scaffolds for engineering replacement tissues and organs. *Biomaterials* 24, 2363–2378 (2003).
18. Nair, L. S. & Laurencin, C. T. Biodegradable polymers as biomaterials. *Prog. Polym. Sci.* 32, 762–798 (2007).
19. Bruce Alberts, Dennis Bray, Julian Lewis, Martin Raff, Keith Roberts, and J. D. W. From Single Cells to Multicellular Organisms. (1994).
20. Roseti, L., Bassi, A., Grigolo, B. & Fornasari, P. M. *Development of Human Chondrocyte – Based Medicinal Products for Autologous Cell Therapy*. (2010).
21. Koh, C. J. Tissue Engineering, Stem Cells, and Cloning: Opportunities for Regenerative Medicine. *J. Am. Soc. Nephrol.* 15, 1113–1125 (2004).
22. Panno, J. *Stem Cell Research: Medical Applications and Ethical Controversy*. (2009).

23. Van der Flier, L. G. & Clevers, H. Stem cells, self-renewal, and differentiation in the intestinal epithelium. *Annu. Rev. Physiol.* 71, 241–60 (2009).
24. Clemens van Blitterswijk, Peter Thomsen, Jeffrey Hubbell, Ranieri Cancedda, Joost de Bruijn, Anders Lindahl, Jerome Sohier, D. F. W. *Tissue Engineering*. 760 (2008).
25. Rippon, H. J. & Bishop, A. E. Embryonic stem cells. *Cell Prolif.* 37, 23–34 (2004).
26. Young, H. E. & Black, A. C. Adult stem cells. *Anat. Rec. A. Discov. Mol. Cell. Evol. Biol.* 276, 75–102 (2004).
27. Ito, Y. Tissue engineering by immobilized growth factors. *Mater. Sci. Eng. C* 6, 267–274 (1998).
28. Shekaran, A. & Garcia, A. J. Nanoscale engineering of extracellular matrix-mimetic bioadhesive surfaces and implants for tissue engineering. *Biochim. Biophys. Acta* 1810, 350–60 (2011).
29. Krishnamoorthy, L., Morris, H. L. & Harding, K. G. Specific growth factors and the healing of chronic wounds. *J. Wound Care* 10, 173–8 (2001).
30. Grazul-Bilska, A. T. *et al.* Wound healing: the role of growth factors. *Drugs Today (Barc).* 39, 787–800 (2003).
31. Andia, I., Sánchez, M. & Maffulli, N. Basic Science: Molecular and Biological Aspects of Platelet-Rich Plasma Therapies. *Oper. Tech. Orthop.* 22, 3–9 (2012).
32. Bennett, N. T. & Schultz, G. S. Growth factors and wound healing: Part II. Role in normal and chronic wound healing. *Am. J. Surg.* 166, 74–81 (1993).
33. Bourque, W. T., Gross, M. & Hall, B. K. Expression of four growth factors during fracture repair. *Int. J. Dev. Biol.* 37, 573–9 (1993).
34. Sinno, H. & Prakash, S. Complements and the wound healing cascade: an updated review. *Plast. Surg. Int.* 2013, 146764 (2013).
35. Schmidt-Bleek, K. *et al.* Inflammatory phase of bone healing initiates the regenerative healing cascade. *Cell Tissue Res.* 347, 567–73 (2012).
36. Verhamme, P. & Hoylaerts, M. F. Hemostasis and inflammation: two of a kind? *Thromb. J.* 7, 15 (2009).
37. Velnar, T., Bailey, T. & Smrkolj, V. The Wound Healing Process: An Overview of the Cellular and Molecular Mechanisms. *J. Int. Med. Res.* 37, 1528–1542 (2009).
38. Robert F. Diegelmann, M. C. E. Wound Healing: An Overview Of Acute, Fibrotic and Delayed Healing Robert F. Diegelmann 1 , and Melissa C. Evans 2 1. 283–289 (2004).
39. Carmeliet, P. & Jain, R. K. Molecular mechanisms and clinical applications of angiogenesis. *Nature* 473, 298–307 (2011).
40. John D. Stroncek and W. Monty Reichert. Overview of Wound Healing in Different Tissue Types. *Front. Neuroeng.* (2008).
41. Sánchez, A. R., Sheridan, P. J. & Kupp, L. I. Is platelet-rich plasma the perfect enhancement factor? A current review. *Int. J. Oral Maxillofac. Implants* 18, 93–103 (2003).
42. Masters, K. S. Covalent growth factor immobilization strategies for tissue repair and regeneration. *Macromol. Biosci.* 11, 1149–63 (2011).
43. Vasita, R. & Katti, D. S. Growth factor-delivery systems for tissue engineering: a materials perspective. *Expert Rev. Med. Devices* 3, 29–47 (2006).
44. Tayalia, P. & Mooney, D. J. Controlled growth factor delivery for tissue engineering. *Adv. Mater.* 21, 3269–85 (2009).
45. Kobsa, S. & Saltzman, W. M. Bioengineering approaches to controlled protein delivery. *Pediatr. Res.* 63, 513–9 (2008).

46. Balasubramanian, V., Onaca, O., Enea, R., Hughes, D. W. & Palivan, C. G. Protein delivery: from conventional drug delivery carriers to polymeric nanoreactors. *Expert Opin. Drug Deliv.* 7, 63–78 (2010).
47. Tang, Y. *et al.* TGF-beta1-induced migration of bone mesenchymal stem cells couples bone resorption with formation. *Nat. Med.* 15, 757–65 (2009).
48. Douglas, H. E. TGF-ß in wound healing: a review. *J. Wound Care* 19, 403–6 (2010).
49. Zhao, L., Jiang, S. & Hantash, B. M. Transforming growth factor beta1 induces osteogenic differentiation of murine bone marrow stromal cells. *Tissue Eng. Part A* 16, 725–33 (2010).
50. Park, H., Temenoff, J. S., Holland, T. A., Tabata, Y. & Mikos, A. G. Delivery of TGF-beta1 and chondrocytes via injectable, biodegradable hydrogels for cartilage tissue engineering applications. *Biomaterials* 26, 7095–103 (2005).
51. Yun, Y.-R. *et al.* Fibroblast growth factors: biology, function, and application for tissue regeneration. *J. Tissue Eng.* 2010, 218142 (2010).
52. Seo, Y.-A. *et al.* Fabrication of highly porous poly (ε-caprolactone) microfibers via electrospinning. *J. Porous Mater.* 19, 217–223 (2011).
53. Murakami, S. Periodontal tissue regeneration by signaling molecule(s): what role does basic fibroblast growth factor (FGF-2) have in periodontal therapy? *Periodontol. 2000* 56, 188–208 (2011).
54. Schmidt, M. B., Chen, E. H. & Lynch, S. E. A review of the effects of insulin-like growth factor and platelet derived growth factor on in vivo cartilage healing and repair. *Osteoarthritis Cartilage* 14, 403–12 (2006).
55. Caplan, A. I. & Correa, D. PDGF in bone formation and regeneration: new insights into a novel mechanism involving MSCs. *J. Orthop. Res.* 29, 1795–803 (2011).
56. Kurten, R. C. *et al.* Coordinating epidermal growth factor-induced motility promotes efficient wound closure. *Am. J. Physiol. Cell Physiol.* 288, C109–21 (2005).
57. Berlanga-Acosta, J. *et al.* Epidermal growth factor in clinical practice - a review of its biological actions, clinical indications and safety implications. *Int. Wound J.* 6, 331–46 (2009).
58. Schultz, G., Chegini, N., Grant, M., Khaw, P. & MacKay, S. Effects of growth factors on corneal wound healing. *Acta Ophthalmol. Suppl. (Oxf.).* 60–6 (1992).
59. Clemmons, D. R. Structural and functional analysis of insulin-like growth factors. *Br. Med. Bull.* 45, 465–80 (1989).
60. Yakar, S., Courtland, H.-W. & Clemmons, D. IGF-1 and bone: New discoveries from mouse models. *J. Bone Miner. Res.* 25, 2543–52 (2010).
61. Govoni, K. E. Insulin-like growth factor-I molecular pathways in osteoblasts: potential targets for pharmacological manipulation. *Curr. Mol. Pharmacol.* 5, 143–52 (2012).
62. Meinel, L. *et al.* Localized insulin-like growth factor I delivery to enhance new bone formation. *Bone* 33, 660–72 (2003).
63. Haase, I., Evans, R., Pofahl, R. & Watt, F. M. Regulation of keratinocyte shape, migration and wound epithelialization by IGF-1- and EGF-dependent signalling pathways. *J. Cell Sci.* 116, 3227–38 (2003).
64. Bao, P. *et al.* The role of vascular endothelial growth factor in wound healing. *J. Surg. Res.* 153, 347–58 (2009).
65. Ferrara, N., Gerber, H.-P. & LeCouter, J. The biology of VEGF and its receptors. *Nat. Med.* 9, 669–76 (2003).
66. Song, S.-Y., Chung, H.-M. & Sung, J.-H. The pivotal role of VEGF in adipose-derived-stem-cell-mediated regeneration. *Expert Opin. Biol. Ther.* 10, 1529–37 (2010).

67. Klein, H. G. and D. J. A. *Mollison's Blood Transfusion in Clinical Medicine*. (2007).
68. Lawrence T. Goodnough, M.D., Mark E. Brecher, M.D., Michael H. Kanter, M.D., and James P. AuBuchon, M. D. Transfusion Medicine — Blood Transfusion. *N Engl J Med* 340:438–447 (1999).
69. Sánchez, M., Andia, I., Anitua, E. & Sánchez, P. Platelet Rich Plasma (PRP) Biotechnology : Concepts and Therapeutic Applications in Orthopedics and Sports Medicine.
70. Intini, G. The use of platelet-rich plasma in bone reconstruction therapy. *Biomaterials* 30, 4956–66 (2009).
71. Civinini, R., Macera, A., Nistri, L., Redl, B. & Innocenti, M. The use of autologous blood-derived growth factors in bone regeneration. *Clin. Cases Miner. Bone Metab.* 8, 25–31 (2011).
72. Wasterlain, A. S., Braun, H. J. & Dragoo, J. L. Contents and Formulations of Platelet-Rich Plasma. *Oper. Tech. Orthop.* 22, 33–42 (2012).
73. Alsousou, J., Thompson, M., Hulley, P., Noble, a & Willett, K. The biology of platelet-rich plasma and its application in trauma and orthopaedic surgery: a review of the literature. *J. Bone Joint Surg. Br.* 91, 987–96 (2009).
74. Cole, B. J., Seroyer, S. T., Filardo, G., Bajaj, S. & Fortier, L. a. Platelet-rich plasma: where are we now and where are we going? *Sports Health* 2, 203–10 (2010).
75. Vogel, J. P. *et al.* Platelet-rich plasma improves expansion of human mesenchymal stem cells and retains differentiation capacity and in vivo bone formation in calcium phosphate ceramics. *Platelets* 17, 462–9 (2006).
76. Kon, E. *et al.* Platelet-rich plasma: intra-articular knee injections produced favorable results on degenerative cartilage lesions. *Knee Surg. Sports Traumatol. Arthrosc.* 18, 472–9 (2010).
77. Sarkar, M. R. *et al.* Bone formation in a long bone defect model using a platelet-rich plasma-loaded collagen scaffold. *Biomaterials* 27, 1817–1823 (2006).
78. Van Bergen, C. J. A. *et al.* Demineralized bone matrix and platelet-rich plasma do not improve healing of osteochondral defects of the talus: an experimental goat study. *Osteoarthritis Cartilage* 21, 1746–54 (2013).
79. Anitua, E., Sánchez, M., Orive, G. & Andia, I. Delivering growth factors for therapeutics. *Trends Pharmacol. Sci.* 29, 37–41 (2008).
80. De Mel, A., Jell, G., Stevens, M. M. & Seifalian, A. M. Biofunctionalization of Biomaterials for Accelerated in Situ Endothelialization: A Review. *Biomacromolecules* 9, 2969–2979 (2008).
81. Ansari, S. A. & Husain, Q. Potential applications of enzymes immobilized on/in nano materials: A review. *Biotechnol. Adv.* 30, 512–23 (2012).
82. Jung, Y., Jeong, J. Y. & Chung, B. H. Recent advances in immobilization methods of antibodies on solid supports. *Analyst* 133, 697–701 (2008).
83. Luginbuehl, V., Meinel, L., Merkle, H. P. & Gander, B. Localized delivery of growth factors for bone repair. *Eur. J. Pharm. Biopharm.* 58, 197–208 (2004).
84. Kalia, J. & Raines, R. T. Advances in Bioconjugation. *Curr. Org. Chem.* 14, 138–147 (2010).
85. Dixit, C. K., Mcdonagh, C., Maccraith, B. D., Biophotonics, N. & Platform, I. Surface Modification and Conjugation Strategies for Bioassay / Biomaterial Applications. (2011).
86. Ungaro, F. *et al.* Bioactivated Polymer Scaffolds for Tissue Engineering.
87. Blackwood, K. a., Bock, N., Dargaville, T. R. & Ann Woodruff, M. Scaffolds for Growth Factor Delivery as Applied to Bone Tissue Engineering. *Int. J. Polym. Sci.* 2012, 1–25 (2012).
88. Cabanas-Danés, J., Huskens, J. & Jonkheijm, P. Chemical strategies for the presentation and delivery of growth factors. *J. Mater. Chem. B* (2013). doi:10.1039/c3tb20853b
89. Hermanson, G. *Bioconjugate Techniques*. 1323 (2008).

90. Staros, J. V, Wright, R. W. & Swingle, D. M. Enhancement by N-hydroxysulfosuccinimide of water-soluble carbodiimide-mediated coupling reactions. *Anal. Biochem.* 156, 220–2 (1986).
91. Mark J. Schulz, Vesselin N. Shanov, Y. Y. *Nanomedicine Design of Particles, Sensors, Motors, Implants, Robots, and Devices (Engineering in Medicine & Biology)*. 511 (Artech House Publishers, 2009).
92. Tsuzuki, S., Wada, A. & Ito, Y. Photo-immobilization of biological components on gold-coated chips for measurements using surface plasmon resonance (SPR) and a quartz crystal microbalance (QCM). *Biotechnol. Bioeng.* 102, 700–7 (2009).
93. Chen, G., Ito, Y. & Imanishi, Y. Photo-immobilization of epidermal growth factor enhances its mitogenic effect by artificial juxtacrine signaling. *Biochim. Biophys. Acta - Mol. Cell Res.* 1358, 200–208 (1997).
94. Ito, Y. Photoimmobilization for microarrays. *Biotechnol. Prog.* 22, 924–32
95. Stefonek-Puccinelli, T. J. & Masters, K. S. Regulation of cell signaling and function via changes in growth factor presentation. *Conf. Proc. IEEE Eng. Med. Biol. Soc.* 2009, 1167–71 (2009).
96. Rouwkema, J., Rivron, N. C. & van Blitterswijk, C. A. Vascularization in tissue engineering. *Trends Biotechnol.* 26, 434–441 (2008).
97. Jain, R. K., Au, P., Tam, J., Duda, D. G. & Fukumura, D. Engineering vascularized tissue. *Nat. Biotechnol.* 23, 821–3 (2005).
98. Alberts B, Johnson A, Lewis J, et al. *Blood Vessels and Endothelial Cells*. (Garland Science, 2002).
99. Hoeben, A. *et al.* Vascular endothelial growth factor and angiogenesis. *Pharmacol. Rev.* 56, 549–80 (2004).
100. Ferrara, N. Binding to the extracellular matrix and proteolytic processing: two key mechanisms regulating vascular endothelial growth factor action. *Mol. Biol. Cell* 21, 687–90 (2010).
101. Miyagi, Y. *et al.* Biodegradable collagen patch with covalently immobilized VEGF for myocardial repair. *Biomaterials* 32, 1280–90 (2011).
102. Shen, Y. H., Shoichet, M. S. & Radisic, M. Vascular endothelial growth factor immobilized in collagen scaffold promotes penetration and proliferation of endothelial cells. *Acta Biomater.* 4, 477–489 (2008).
103. Chiu, L. L. Y., Weisel, R. D., Li, R. & Radisic, M. Defining conditions for covalent immobilization of angiogenic growth factors onto scaffolds for tissue engineering. 69–84 (2011). doi:10.1002/term
104. Chiu, L. L. Y. & Radisic, M. Scaffolds with covalently immobilized VEGF and Angiopoietin-1 for vascularization of engineered tissues. *Biomaterials* 31, 226–241 (2010).
105. Saik, J. E., Gould, D. J., Watkins, E. M., Dickinson, M. E. & West, J. L. Covalently immobilized platelet-derived growth factor-BB promotes angiogenesis in biomimetic poly(ethylene glycol) hydrogels. *Acta Biomater.* 7, 133–43 (2011).
106. Fonder, M. A. *et al.* Treating the chronic wound: A practical approach to the care of nonhealing wounds and wound care dressings. *J. Am. Acad. Dermatol.* 58, 185–206 (2008).
107. Goldman, R. Growth factors and chronic wound healing: past, present, and future. *Adv. Skin Wound Care* 17, 24–35
108. Puccinelli, T. J., Bertics, P. J. & Masters, K. S. Regulation of keratinocyte signaling and function via changes in epidermal growth factor presentation. *Acta Biomater.* 6, 3415–3425 (2010).
109. Keller, G. Embryonic stem cell differentiation: emergence of a new era in biology and medicine. *Genes Dev.* 19, 1129–55 (2005).
110. Leipzig, N. D., Wylie, R. G., Kim, H. & Shoichet, M. S. Differentiation of neural stem cells in three-dimensional growth factor-immobilized chitosan hydrogel scaffolds. *Biomaterials* 32, 57–64 (2011).

111. Rahman, N., Purpura, K. A., Wylie, R. G., Zandstra, P. W. & Shoichet, M. S. The use of vascular endothelial growth factor functionalized agarose to guide pluripotent stem cell aggregates toward blood progenitor cells. *Biomaterials* 31, 8262–70 (2010).
112. Schuldiner, M., Yanuka, O., Itskovitz-Eldor, J., Melton, D. A. & Benvenisty, N. Effects of eight growth factors on the differentiation of cells derived from human embryonic stem cells. *Proc. Natl. Acad. Sci. U. S. A.* 97, 11307–12 (2000).
113. Temenoff, J. S. & Mikos, A. G. Review: tissue engineering for regeneration of articular cartilage. *Biomaterials* 21, 431–440 (2000).
114. Tang, Q. O. *et al.* TGF-beta3: A potential biological therapy for enhancing chondrogenesis. *Expert Opin. Biol. Ther.* 9, 689–701 (2009).
115. Deyo, R. A. *et al.* Use of bone morphogenetic proteins in spinal fusion surgery for older adults with lumbar stenosis: trends, complications, repeat surgery, and charges. *Spine (Phila. Pa. 1976).* 37, 222–30 (2012).
116. Garrison, K. R. *et al.* Clinical effectiveness and cost-effectiveness of bone morphogenetic proteins in the non-healing of fractures and spinal fusion: a systematic review. *Health Technol. Assess.* 11, 1–150, iii–iv (2007).
117. Boyne, P. J. Application of Bone Morphogenetic Proteins in the Treatment of Clinical Oral and Maxillofacial Osseous Defects. *J. Bone Jt. Surg.* 83, S146–S150 (2001).
118. Shen, H., Hu, X., Yang, F., Bei, J. & Wang, S. The bioactivity of rhBMP-2 immobilized poly(lactide-co-glycolide) scaffolds. *Biomaterials* 30, 3150–7 (2009).
119. Park, Y. J. *et al.* Immobilization of bone morphogenetic protein-2 on a nanofibrous chitosan membrane for enhanced guided bone regeneration. *Biotechnol. Appl. Biochem.* 43, 17–24 (2006).
120. Zhang, H., Migneco, F., Lin, C.-Y. & Hollister, S. J. Chemically-conjugated bone morphogenetic protein-2 on three-dimensional polycaprolactone scaffolds stimulates osteogenic activity in bone marrow stromal cells. *Tissue Eng. Part A* 16, 3441–8 (2010).

Chapter 2 Materials and Methods

Chapter 2

Materials and Methods

The aim of this chapter is to describe, in detail, the materials used and the experimental methods carried out to achieve the experimental results presented below. Also, this chapter will provide some insights on the methodological fundaments to properly justify the methods selected to answer specific research questions of this experimental work.

2.1 Materials

Polycaprolactone (PCL; Mw = 70 000 – 90 000 determined by GPC), Chloroform and N,N-Dimethylformamide (DMF) were purchased to Sigma Aldrich, kept at room temperature and use as received. PLC belongs to the aliphatic polyester family, being characterized by good mechanical/elastic properties, low toxicity, biocompatibility and long-term biodegradability. Anti-human TGF-β1 monoclonal antibody was purchased from PrepoTech Inc. (Rochy Hill, NJ; USA), reconstituted in sterile water and kept at -20°C until further use. Recombinant bFGF oligoclonal antibody (clone 7HCLC), was purchased from Life Technologies (Carlsbad, CA; USA), reconstituted in a phosphate buffer solution (PBS) and kept at -20°C until further use. VEGF (JH121) antibody was purchased from Santa Cruz Biotechnology Inc. (USA) and kept at 4°C until further use. All these antibodies have specific reactivity to human samples, and the host of the VEGF and the TGF-β1 antibodies was mouse, and for the bFGF antibody the host was a rabbit. Regarding the secondary antibodies, both Alexa Fluor® 488 donkey anti-rabbit IgG (H+L), with green fluorescence, and Alexa Fluor® 594 goat anti-mouse IgG (H+L), with red fluorescence, were purchased from Life Technologies (Carlsbad, CA; USA) and kept at 4°C until further use. Alexa Fluor® 488 was used to recognize the immobilized bFGF antibody, whereas the Alexa Fluor® 594 was used to recognize the immobilized TGF-β1 and VEGF antibodies.

Growth Factors (GFs), namely the recombinant human TGF-β1 (a protein composed of two identical 112 amino acid polypeptide chains linked by a single disulfide bond) and basic-FGF (a protein consisting of 154 amino acid residues) were expressed in *Escherichia coli*, whereas the recombinant human $VEGF_{121}$ (a disulfide-linked homodimeric protein

consisting of two 121 amino acid polypeptide chains) was expressed in *CHO cells*, all purchased from PrepoTech Inc. (Rochy Hill, NJ; USA), reconstituted in sterile water and kept at -20°C until further use.

2.2 Methods

2.2.1 Scaffold Fabrication and (Bio)Functionalization

2.2.1.1 The processing technique Electrospinning

The PCL nanofiber meshes (NFMs) were produced by the electrospinning technique. This processing methodology is an efficient and versatile technique used to produce ultrafine fibers ranging from nano- to micro-scales The methodology and the phenomena behind this processing technique has been extensively described [1,2]. The typical electrospinning setup consists in a spinneret coupled to a polymeric solution reservoir, a high voltage power source and a collector, as depicted in **Figure 2.1**. Electrospinning involves the application of a high voltage to the polymeric solution, resulting in the ejection of the solution through the needle. Basically, this electrostatic force opposes the surface tension of the solution causing the initiation of a jet. As this jet travels from the needle to the collector, the solvent partially evaporates and a fiber mesh is formed in a defined conductive collector [1,2].

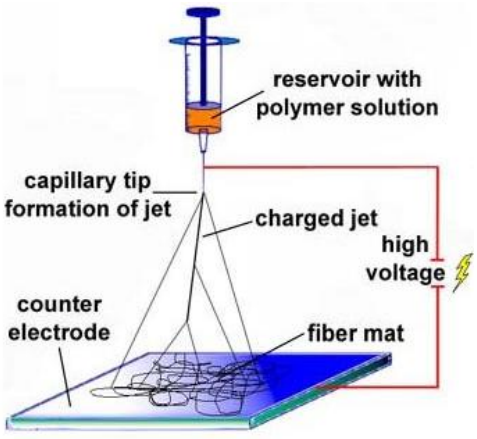

Figure 2.1 Electrospinning setup composed by an electric power supply, a syringe pump and collector.

For the production of the PCL NFMs, a 5 mL plastic syringe (B-Braun) and a needle with 0.8 mm circular external diameter tip was used to electrospun the PCL solution. A 17%

(w/v) PCL solution was prepared with an organic solvent mixture composed of Chloroform and DMF, in a 7:3 ratio as described elsewhere [3]. Briefly the PCL solution was left to mix in the stirrer overnight. The mesh was electrospun by applying a voltage of 13.6 kV, a needle tip-to-tip to ground collector distance of 18 cm and a flow rate of 1mL/h. After the complete processing of a 1mL of solution, the NFM was left to dry for 1 day, to make sure that all solvent residues had been evaporated. The processed NFM was further cut into smaller samples of 1cm x 1cm for further assays.

The produced PCL NFMs are characterized by a high specific surface area that in combination with the microporous structure facilitates cell adhesion, proliferation, migration and differentiation. NFMs are typically distinguished to mimic the extracellular matrix of many tissues, by imitating its fibrils morphology and by the diameter of the fibers, providing an adequate 3D microenvironment for cell-cell and cell-biomaterial interactions. All these physical properties are of great importance when considering the TE strategies [4]. PCL is a biodegradable polyester with hydrophobic properties. Recently PCL had gained particular interest in research due to its potential use as a biomaterial mainly related with its biocompatibility and low toxicity and it is already used in clinical for very applications including resorbable sutures.

2.2.1.2 Surface Functionalization of Electrospun Nanofibers

PCL does not have amine functional groups, thus its surface needs to be activated, for further insertion of amine group. The activation of the surface was obtained by an ultraviolet-ozone (UV-O) irradiation (UV-O Cleaner®, model ProCleaner 220 from Bioforce Nanoscience). The UV-O method is a photo-sensitized oxidation process in which the molecules are excited and/or dissociated by the absorption of short-wavelength UV radiation. The products of this excitation reaction with atomic oxygen form simpler volatile molecules which desorbs from the surface. When both UV wavelengths (184.9 nm and 253.7 nm) are presented, atomic oxygen (O) is continuously generated, as well as ozone is formed and destroyed, simultaneously.

Both sides of the NFMs were exposed during 4 minutes to UV-O irradiation, as previously optimized [5] . After this surface activation, amine groups were inserted (-NH_2) at the surface of the electrospun meshes. It is possible that the amine groups can be introduced

onto the PCL surface by a reaction with diamine (e.g. hexamethylenediamine (HMD)), providing that one amine group reacts with the -COOH- group of the PCL to form a covalent bound, while the other amine group is unreacted and freely. Therefore, PCL NFMs were immersed in a 1 M HMD (Sigma Aldrich) solution during 1h at 37°C. The amount of $-NH_2$ (2.83 ± 0.11 nmol/cm^2) was determined indirectly by quantifying the amount of free –SH groups according to Ellman's reagent method [5]. Both treatments decreased the hidrophobicity of the electrospun NFM, affecting also the nanofiber mesh structure by breaking some of top fibers of the mesh, as it is visible in **Figure 2.2 b)**. The uniformity in fiber diameter seems also to be affected by the treatment.

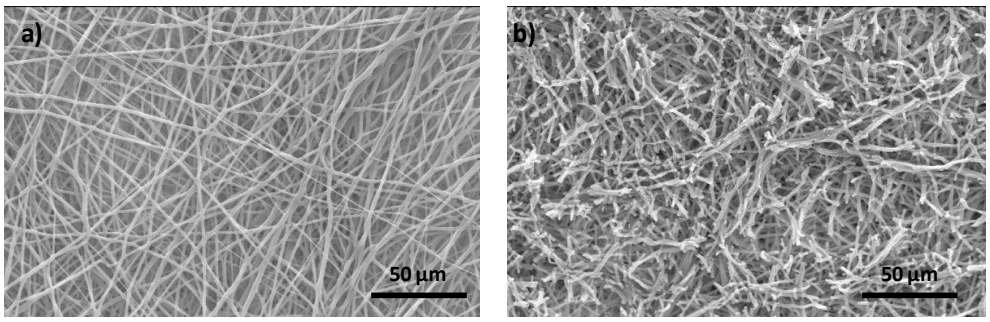

Figure 2.2 SEM analysis of an electrospun PCL NFM at 500X magnification: a) not subjected to any physicochemical treatment and b) after UV-ozone and aminolysis functionalization.

2.2.2 Antibodies Immobilization Strategy

The main concept of this work is the immobilization of specific GFs from a pool of different proteins and GFs. One possible route to immobilize the GF of interest involves the use of antibodies as an intermediate linker. Antibodies or immunoglobulins are Y-shaped proteins produced by B-cells and used by the immune system to identify and neutralize foreign objects such as bacteria and viruses, by recognizing a unique part of the foreign target [6].

Antibodies have two different regions: a variable region that is specific of each antibody and a non-variable region that is common for each type of antibody **(Figure 2.3**). The specific and variable region is also known as the antigen binding site where only a specific antigen (GFs in the present case) can be linked.

Typically, there is a carboxyl group (-COOH) in the antibodies structure at the end of their non-variable region. This group is used to react with the amine groups (-NH_2) that were previously inserted at the surface of electrospun nanofibers, leading to the covalent immobilization of an antibody to the polymeric substrate. This covalent immobilization step often requires a linker to achieve a more stable and strong binding. In the present work, the EDC/NHS (1-Ethyl-3-[3-dimethylaminopropyl]carbodiimide hydrochloride/ N-hydroxysuccinimide) (Sigma Aldrich) combination was used as a linker since it is one of the most widely reported linkers that enhances the efficiency of the immobilization.

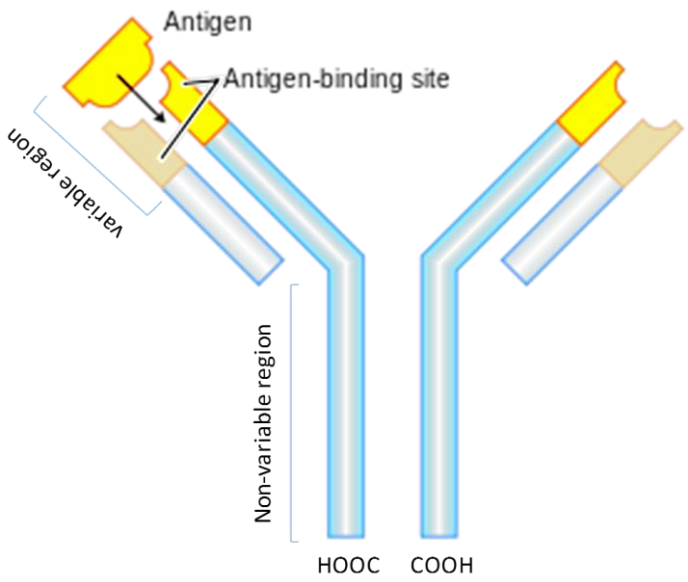

Figure 2.3 The antibody structure, representing the variable and the non-variable region, as well as the carboxyl group at the end of the former region.

The required steps to immobilize an antibody at the surface of electrospun nanofibers, for further binding of the corresponding GFs from the PL are shown in **Figure 2.4**. After the surface functionalization of the nanofibers by UV-O and aminolysis each electrospun mesh was placed in a 24 well-plate and the primary antibody was mixed with EDC/NHS for 15 min at RT, to activate the antibody. This primary antibody solution was further added to each functionalized electrospun NFM. After overnight incubation, this solution was removed and the NFMs were washed with PBS. Then, a 3% BSA blocking step was performed for 30 minutes at RT. The BSA solution was removed and the secondary antibody was added to determine the degree of immobilization (indirect method was used by quantifying the fluorescence of unbound secondary antibody). The fluorescent-labeled

secondary antibody was incubated for 1h at RT, and the fluorescence of the remaining solution was read out in a MicroPlate Reader (Synergy HT, BioTek). The different specimens of each sample were washed and reserved in PBS at 4°C and kept in the dark, until fluorescent microscopy observation. Parallel experiments were performed to assess the binding efficiency of recombinant proteins and PL-derived proteins to antibodies. All the previous described steps were conducted expect the secondary antibody step that was replaced by adding these solutions (recombinant protein and PL samples) and incubating them during 1h at RT. Samples of recombinant proteins and from PL were kept and frozen until ELISA quantification.

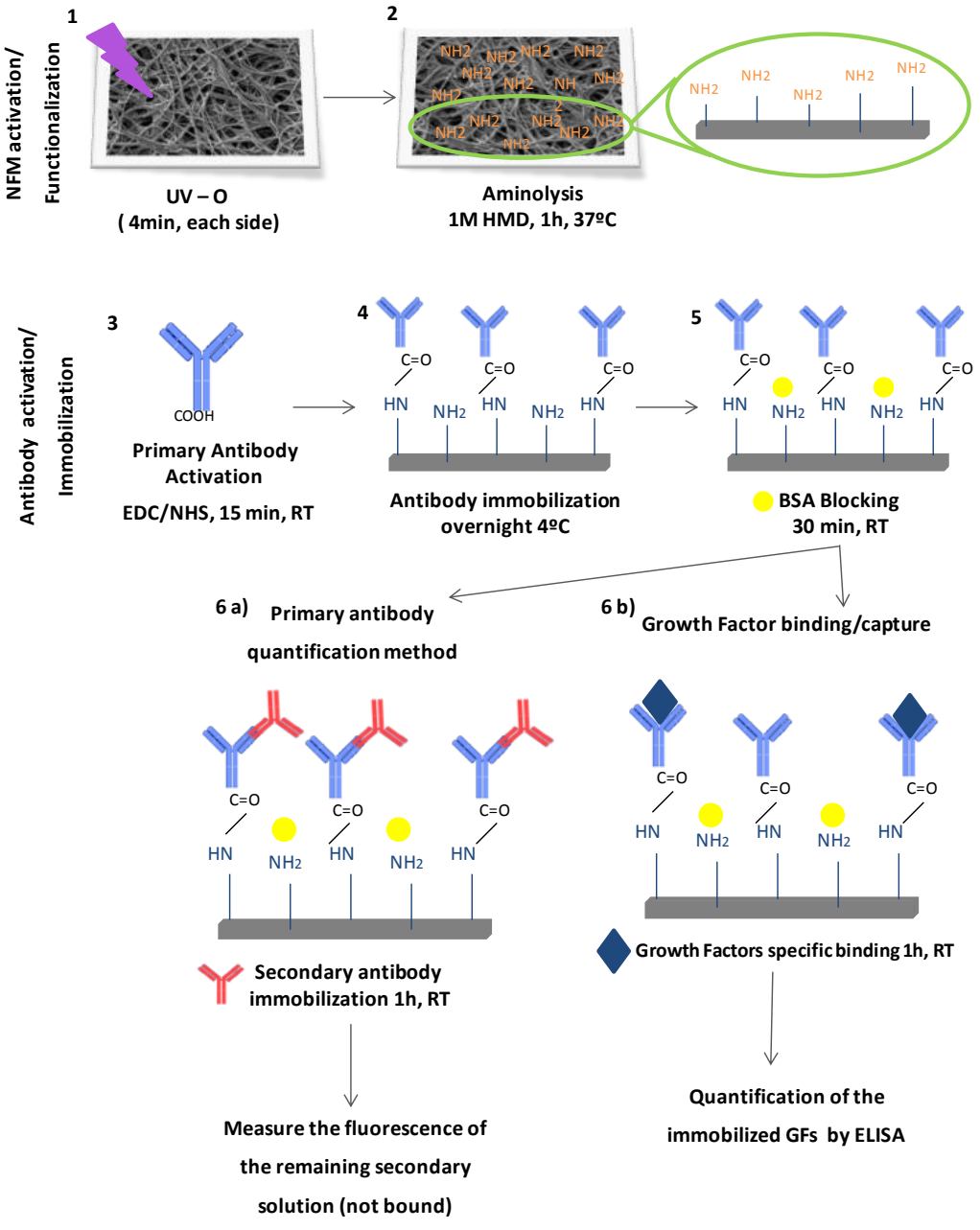

Figure 2.4 Antibody and antigen immobilization strategy, applied to the electrospun PCL NFMs, for further detection by the fluorescence reading method (sequence of steps required)

2.2.2.1 EDC/NHS ratio and concentration optimization

EDC couples carboxyl groups to primary amines. Although NHS (N-hydroxysuccinimide) is not required for carbodiimide reactions, its use greatly enhances the coupling efficiency, leading to a two-step reaction (**Figure 2.5**). With the combination of EDC/NHS, amine reactive NHS esters can be available to react with any carboxyl-containing molecule (-COOH) [7].

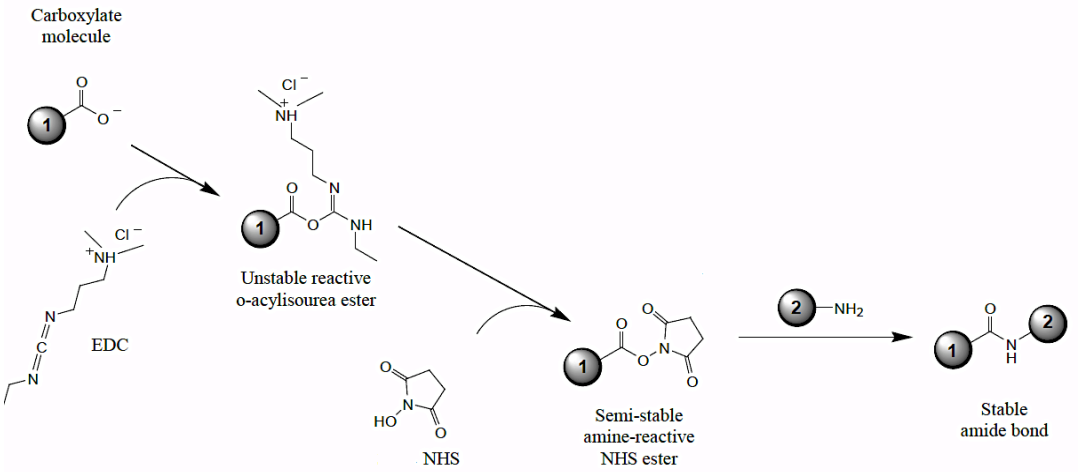

Figure 2.5 EDC reacts preferentially with the carboxyl groups forming O-acylisourea, an unstable reactive ester. In combination with NHS forms a semi-stable amine-reactive ester. This NHS ester can readily react with the available amine groups at the surface of electrospun nanofibers.

EDC/NHS was dissolved in 0.1 MES(2-N-morpholino) ethanesulfonic acid) buffer with 0.9% (wt/wt) NaCl, following pH adjustment to pH=4.7. To optimize the reactive action of this linker, three different parameters were tested: the ratio between EDC and NHS, the concentration of the EDC and NHS, and their final concentration in the primary antibody solutions. For the testing of the first parameter, five different EDC/NHS ratios were tested, i.e. 1:4, 1:2, 1:1, 2:1 and 4:1. After selecting the best EDC/NHS ratio, the next step was to test their concentrations. In this assay, four different concentrations were studied: 10mM EDC + 40 mM NHS, 26 mM EDC + 104 mM NHS, 50 mM EDC + 100 mM NHS and 100 mM EDC + 400 mM NHS. With the optimized reaction conditions in terms of EDC/NHS ratio and respective concentrations, the final concentration of the linker in the antibody solution was assessed to the 1%, 5% and 10% concentrations. The optimized conditions for those

three parameters (1:4 ratio; 50 mM EDC + 200 mM NHS concentration and 1% concentration) were the ones used in all further experiments.

2.2.2.2 Optimization of Single Antibody Immobilization and Determination of the Standard Curves

Three different antibodies were immobilized (anti-TGF-β1, anti-bFGF and anti-VEGF) at the surface of the activated and functionalized electrospun nanofiber meshes. A wide range of primary antibody concentrations (from 0 μg/mL to 20 μg/mL) was tested in order to find the maximum immobilization capacity of the system. The electrospun NFMs were placed in 24 well-plates and 200 μl of each primary antibody concentration was added to each well/meshes. After overnight incubation at 4 °C, each mesh was washed twice with 300 μl 0.1 M PBS (5 min each time) and a blockage of 3% BSA was performed for 30 minutes at RT. The BSA solution was removed and the secondary antibody (1:200 in PBS) incubated for 1h at RT. A microplate reading (Synergy HT-BioTek) was performed to quantify the fluorescence of unbound secondary antibody solution (n=3 samples, read in triplicate). For the TGF-β1 and VEGF antibodies, Alexa Fluor® 594 was used and the reading parameters were the following absorption at 590 nm and the emission at 617 nm. In the case of the anti-bFGF, the selected secondary antibody was the Alexa Fluor® 488 and the reading parameters were 495 nm for the adsorption and 519 nm for the emission spectrum. Negative control samples were also prepared, where all antibody immobilization steps were performed with the exception of the primary antibody incubation, which was substituted by PBS.

In further experiments, the following optimized primary antibody concentrations were use: 4 μg/mL for anti-VEGF, 8 μg/mL for bFGF and 12 μg/mL for TGF-β1. To define the standard curve of each primary antibody, five concentrations were used to define a linear regression with a R^2 always above 0.98.

2.2.2.3 Mixed immobilization of two antibodies (VEGF and bFGF)

With the attempt to demonstrate the possibility to immobilize more than one antibody in the same polymeric substrate, VEGF and bFGF antibodies were selected. To achieve this purpose, both antibodies were mixed in the same PBS solution at the concentrations optimized before, for a final volume of 200 μl solution per mesh. The antibodies mixture was incubated overnight at 4°C and then the samples were washed twice with 0.1 M PBS (5

minutes each) and a 3% BSA incubation step for 30 min at RT was performed to block all the non-specific sites. The BSA solution was removed and the secondary antibody Alexa Fluor® 594 (for anti-VEGF) was incubated for 1h at RT. The exceeding secondary antibody solution was collect for further quantification (n=3 samples, read in triplicate), as previously described, and the sample washed twice. The same approach was carried out for the secondary antibody Alexa Fluor® 488 (for anti-bFGF). Both secondary antibodies were prepared in a 1:200 concentration, diluted in PBS. A negative control sample was performed, without the immobilization of the primary antibodies, although all the other steps were done to allow observing the samples under laser scanning confocal microscopy.

2.2.2.4 Side-by-side immobilization of two antibodies

The side-by-side immobilization aimed to immobilize distinct antibodies in different areas of the same polymeric substrate. To achieve that purpose, a compartmental watertight chamber (**Figure 2.6**) was developed capable of physically divide a single 1cmx2cm functionalized electrospun NFM into two distinct areas, without the mixture of different solutions and respective antibodies. A device made of acrylic was developed, with 4 cm of external diameter and an internal chamber where the membrane was inserted. A compartmental watertight ring made of expanded Polyvinl Chloride (PVC), with a separation bar that allows the physical division of the electrospun NFM into two areas, is placed on top of the functionalized electrospun NFM. The chamber is sealed with 4 screws so that the compartmental ring makes pressure over the NFM and does not allow the solutions to diffuse from one side to the other. Two different antibody solutions containing VEGF and bFGF, were prepared at the concentrations described above and dropped over each side of the functionalized electrospun NFM. All the antibody immobilization steps (washings, BSA blocking and secondary antibody incubation) were performed, as previously described for the single antibody immobilization. The quantification of unbound secondary antibody was also performed and the samples recovered to characterize the spatial distribution of the antibodies by laser scanning confocal microscope.

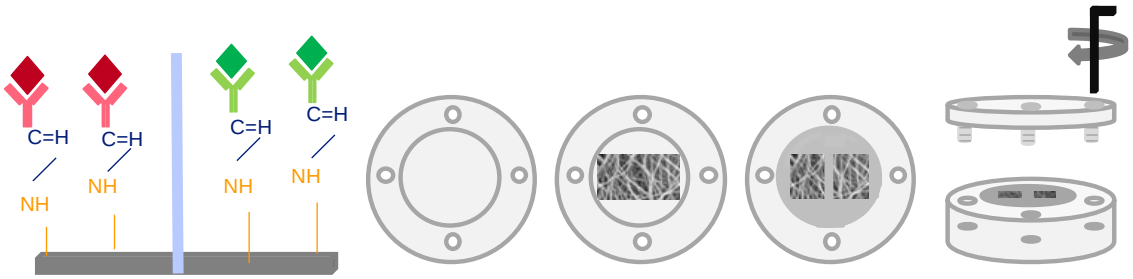

Figure 2.6 Schematic representation of the compartment watertight device, that allows the simultaneous immobilization of two different antibodies in two areas of a single mesh.

2.2.2.5 Laser Scanning Confocal Microscopy

Laser Scanning Confocal Microscopy was conducted in order to characterize the spatial distribution of the antibodies at the surface of the electrospun PCL NFMs. In this technique, the biological molecules are labeled with a fluorescence maker (in this case Alexa Fluor® 594 and 488) and detected visually by selecting an appropriate wavelength (excitation at 495 nm for Alexa® 488 and 590 nm for Alexa 594). Emission at 570 nm for the red channel and at 540 nm for the green channel). In confocal microscopy, a laser beam is split and refocused just on the plane of interest. This reduces one problem of normal fluorescence microscopy where the entire sample is illuminated and both in-focus and out-of-focus points contribute equally to the signal. The greatest advantage is the possibility of making three-dimensional maps of the samples to within a depth of around 100-200 μm. This is particularly relevant to demonstrate immobilized antibodies in PCL NFMs. The antibodies were immobilized as previous described and single (TGF-β1, bFGF and VEGF) and multiple (mixed or side-by-side designs) samples were placed in glass slides and analyzed by laser scanning confocal microscopy (FluoView 1000, Olympus, Germany) at a 10x magnification.

2.2.3 Recombinant and PL-derived growth factor quantification

2.2.3.1 Platelets Lysate: Preparation and Activation

Platelet Rich Plasma (PRP) was provided by "Instituto Português do Sangue", which certifies the biological product according to the Portuguese legislation. The number of platelets was counted and the sample volume is adjusted to 1 million platelets per μL. At the

3B´s cell culture lab, the collected PRP samples were subjected to a 3 repeating temperature-shock cycles (frozen with liquid nitrogen at −196°C and further heated at 37 °C) and the remaining platelets were eliminated by centrifugation. A pool of Platelet Lysate (PL) was stored at -20°C until further use. At the time of each experiment PL solution was thawed and filtered with a 0.22 µm filter.

2.2.3.2 Fluorescence-Linked immunosorbent Assay (FLISA)

After optimizing the maximum concentration of immobilized antibody, the loading capacity of the correspondent GF was tested. For that, both the corresponding recombinant proteins and the PL were tested for each biofunctionalized system. Basically, after all the antibodies immobilization steps previously described, 200 µl of the recombinant protein solutions at different concentrations (ranging from 0 µg/mL to the concentration of each primary antibody) were incubated for 1h at RT. The unbounded recombinant protein solutions were collected and stored at -20°C until further analysis. Two PBS washing steps (5 minutes each) were made and the biofunctionalized systems were incubated overnight at 4°C with the corresponding primary antibody. After removal of the exceeding primary antibody solutions, the biofunctionalized systems were washed again with PBS, another BSA blocking step was performed and the correspondent secondary antibody was incubated for 1 hour at RT. The fluorescence of unbounded secondary solutions was read at the microplate reader, in order to quantify the secondary antibody that has not been immobilized. When PL was used as the source of GFs, the same procedure was followed, although the recombinant protein solution was substituted by 200 µl of PL solution.

2.2.3.3 Enzyme-Linked Immunosorbent Assay (ELISA)

A complementary analysis was performed to access the amount of unbounded GFs, after incubation with biofunctionalized systems comprising antibodies immobilization. The original recombinant protein and PL solutions, before their incubation with the functionalized systems, were also stored at -20°C and used to quantify the initial amount of GFs. For the GFs quantification, human basic-FGF and VEGF development ELISA kits were purchased from PrepoTech (Rochy Hill, NJ; USA) and stored at -20°C, whereas the human TGF-β1 ELISA kit was bought from Boster Biological Technology (Fremont, Ca; USA) and kept at 4°C

until further use. bFGF and VEGF development ELISA kits were a two-days procedure. In the first part, the primary antibody was added to the 96 well-plate (Nunc-Immuno™ MicroWell™ 96 well solid plates, Sigma Aldrich) and left over night in order to be immobilized at the wells bottom. All solutions were prepared according to the manufacturer protocol. Briefly, four washing steps were made and a 1% BSA blocking step for 1h was performed. Both standards (0-1 ng/mL for VEGF and 0-4 ng/mL for bFGF) and samples were added in triplicate (100 µl) and incubated for 2 hours at RT. Another washing step was made and the detection antibody was left to incubate also for 2 hours. The plate was aspirated and washed, an Avidin-horseradish peroxidase (HRP) conjugate was added in a 1:2000 concentration and left to incubate for 30 minutes at RT. 100 µl of an 2,2'-azino-bis(3-ethylbenzthiazoline-6-sulphonic acid (ABTS) liquid substrate was added to each well, and the plate was read at 405 nm and 650 nm.

The TGF-β1 ELISA is a ready-to-use kit, where the plate has been previously coated with the antibody. Briefly, 100 µl of the standards (ranging from 0 pg/ml to 1000 pg/ml) and samples were added to each well and incubated for 1 hour and 30 minutes at 37°C. The content was discarded and 100 µl of biotinylated human TGF-β1 antibody working solution was added to each well and incubated for 1h at 37°C. The plate was washed 3 times with 0.01 M PBS and 100 µl of the Avidin-Biotin-Peroxidase complex (ABC) working solution was added to each well and incubated for 30 minutes at 37°C. The plate was then washed five times with PBS and 90 µl of TMB color developing agent was added to each well and incubated in the dark for 20-25 minutes. 100 µl of the TMB stop solution was added to each well and the color changed to yellow. The absorbance at 450 nm was read in the microplate reader (Synergy HT, Bio-TEK).

2.2.4 Biological Part

2.2.4.1 Cell culture and seeding

A human pulmonary microvascular endothelial cell line (HPMEC-ST1.6R) was used to validate the developed biofunctionalized nanofibrous substrate. This cell line is used to study *in vitro* angiogenic process [8].

HPMEC-ST1.6R cells [8] were cultured with M199 medium (Sigma Aldrich) supplemented with 20% FBS (Alfagene), 2 mM Glutamax (Life Technologies), Pen/Strep (100

U/100 g/mL; Life Technologies), heparin (50 µg/mL; Sigma Aldrich), Endothelial cell growth supplement (ECGS - 25 µg/mL; Becton Dickinson) and incubated at 37°C in a humidified 5% CO_2 atmosphere. HPMEC-ST1.6R cells were used at passages 30-32. Medium was changed twice a week until cell reached 90% of confluence. Then cells were harvested and seeded onto the activated and functionalized electrospun NFMs.

The electrospun PCL NFMs were sterilized by ethylene oxide at Pronefro® Produtos Nefrológicos, S.A. (Porto, Portugal). For NFM_AB1, NFM_Ab2, NFM-$VEGF_{Rec}$ and NFM+$VEGF_{PL}$, VEGF antibody was immobilized overnight and, after the BSA blocking step, human recombinant protein, human recombinant protein (VEGF=4 µg/mL) and PL were incubated. Cell seeding was performed by dropping a 50 µl cell suspension containing 50 000 cells per substrate and left overnight. After cell attachment, culture medium was added to each type of cells and conditions. Untreated electrospun PCL NFMs and NFMs where nanofibers were subjected to surface activation, aminolysis and primary antibody immobilization were used as controls. After 1, 3 and 7 days of culture, samples were collected for cell viability assay, DNA and total protein quantification and VEGF quantification.

2.2.4.2 Cell Viability

The MTS assay is a colorimetric method commonly used for cytotoxicity assays or for determining the number of viable cells in proliferation. The MTS assay is based on bioreduction of a novel tetrazolium compound, 3-(4.5-dimethylthiazol-2-yl)-5-(3-carboxymethoxyphenyl)-2-(4-sulfofenyl)-2H-tetrazolium [MTS], into a brown formazan product that is soluble in tissue culture medium. The quantity of formazan product, as measured by the amount of 490 nm absorbance, is directly proportional to the number of living cells in culture [9].

The metabolic activity of HPMEC-ST1.6R cells seeded on untreated electrospun PCL NFM, NFMs with primary antibody immobilization, and biofunctionalized nanofibrous substrates (recombinant and PL-derived) was determined by the MTS assay (CellTiter 96 ® AQ_{ueous} One Solution, Promega). Basically, at days 1, 3 and 7, the culture medium was removed and the samples were rinsed with sterile PBS. A mixture of culture medium and MTS reagent (5:1 ratio) was added to each mesh, as well as to the negative control comprising no cells or samples. All conditions were performed in triplicate and left to incubate for 3h, at 37 °C in a humidified 5% CO_2 atmosphere. Thereafter, the absorbance of

the MTS reaction medium from each sample was read in triplicate at 490 nm in a microplate reader (Synergy HT, Bio-TEK).

2.2.4.3 Cell Proliferation

The accurate determination of DNA concentration is essential for many processes in molecular biology and physiology [10]. Cell proliferation was determined by using a fluorimetric dsDNA quantification kit (Quant-iT™, PicoGreen®, Molecular Probes, Invitrogen, USA). The samples were collected at days 1, 3 and 7, washed twice with sterile PBS and transferred into eppendorf tubes containing 1 mL of ultrapure water. These samples were frozen at -80 °C until further analysis. Prior to DNA quantification, the various specimens for each sample were thawed and sonicated for 15 min. DNA standards were prepared at concentrations ranging from 0 to 2 μg/mL. Per each well of an opaque 96-wells plate (Falcon) were added 28.7 μL of sample or standard (n=3), 71.3 μL of PicoGreen solution and 100 μL of TE buffer. The plate was incubated for 10 min in the dark and the fluorescence was measured in a microplate reader (Synergie HT, Bio-Tek; USA) by using an excitation wavelength of 480 nm and an emission wavelength of 528 nm. The DNA concentration of each sample was calculated using a standard curve relating DNA concentration and fluorescence intensity.

2.2.4.4 Total Protein synthesis

Samples were collected and prepared for assaying, as previously described in the Cell Proliferation. For the quantification of total protein synthesis, a Micro BCA™ Protein Assay Kit (Pierce, Thermo Scientific) was used. The assay was made accordingly to the manufacturer instructions. Briefly, standards were prepared at various concentrations ranging from 0 μg/mL to 40 μg/mL in ultra pure water. 150 μL of both samples and standards were assayed in triplicate and 150 μl of working reagent were further added to each 96-well plate. The plate was sealed and incubated for 2 hours at 37 °C. The plate was left to cool down to RT and, thereafter, the absorbance at 562 nm was measured in a microplate reader (Synergy HT, Bio-Tek).

2.2.4.5 Statistical analysis

Statistical analysis was performed using Graph Pad Prism Software. Differences between the different conditions of the cellular assays were analyzed using non-parametric test (Kruskal-Wallis test) and a $p<0.05$ was considered significant. Data were presented as mean ± standard deviations.

2.3 References

1. Martins, a., Reis, R. L. & Neves, N. M. Electrospinning: processing technique for tissue engineering scaffolding. *Int. Mater. Rev.* 53, 257–274 (2008).
2. Pham, Q. P., Sharma, U. & Mikos, A. G. Electrospinning of polymeric nanofibers for tissue engineering applications: a review. *Tissue Eng.* 12, 1197–211 (2006).
3. Martins, A. *et al.* Surface modification of electrospun polycaprolactone nanofiber meshes by plasma treatment to enhance biological performance. *Small* 5, 1195–206 (2009).
4. Dhandayuthapani, B., Yoshida, Y., Maekawa, T. & Kumar, D. S. Polymeric Scaffolds in Tissue Engineering Application: A Review. *Int. J. Polym. Sci.* 2011, 1–19 (2011).
5. Monteiro N., Martins A., Pires R. A., Faria S., Fonseca N. A., Moreira J. N., Reis R. L., and N. N. M. *Immobilization of bioactive factor-loaded liposomes at the surface of electrospun nanofibers targeting tissue engineering strategies*. (2013). doi:10.1002/term.1822
6. Charles A Janeway; Paul Tavers, M. W. & M. J. S. Immunobiology. (2001).
7. Fischer, M. J. E. Surface Plasmon Resonance. 627, 55–74 (2010).
8. Krump-Konvalinkova, V. *et al.* Generation of Human Pulmonary Microvascular Endothelial Cell Lines. *Lab. Investig.* 81, 1717–1727 (2001).
9. Buttke, T. M., McCubrey, J. A. & Owen, T. C. Use of an aqueous soluble tetrazolium/formazan assay to measure viability and proliferation of lymphokine-dependent cell lines. *J. Immunol. Methods* 157, 233–240 (1993).
10. Ahn, S. J., Costa, J. & Emanuel, J. R. PicoGreen quantitation of DNA: effective evaluation of samples pre- or post-PCR. *Nucleic Acids Res.* 24, 2623–5 (1996).

Chapter 3

Biofunctional Nanofibrous Substrate Comprising Immobilized Antibodies and Selective Binding of Autologous Growth Factors

Biofunctional Nanofibrous substrate comprising immobilized antibodies and selective binding of autologous growth factors

Abstract

The immobilization of biomolecules at the surface of different biomedical devices has attracted enormous interest, in order to enhance their biological functionality at the cellular level. This work aims to develop a biofunctional polymeric substrate capable of selectively bind Growth factors (GFs) of interest from a pool of proteins present in a biological fluid: Platelet Lysate (PL). Different antibodies were previously immobilized at the substrate surfaces, taking advantage of the specific binding between an antibody and its correspondent antigen. To achieve that purpose, the surface of electrospun PCL nanofibers were activated and functionalized in order to insert chemical groups for the immobilization of antibodies. After determining the maximum immobilization capacity of each antibody: TGF-β1 (12 μg/mL), bFGF (8 μg/mL) and VEGF (4 μg/mL) the next step was to bind the correspondent GF. Using recombinant proteins almost 100% of the initial concentration was immobilized, whereas for PL-derived GFs the efficiency was of 84 - 87% for TGF-β1, 55 - 64% for bFGF and 50 - 59% for VEGF. With this immobilization method we succeeded in developing a platform for the quantitative measurement of either natural or recombinant proteins in a wide and higher efficiency than the ones already available. Cellular assays confirmed that the biological activity of the bound VEGF (both recombinant and PL-derived). Multiple antibodies (i.e. bFGF and VEGF) were also immobilized over the same structure in a mixed or side-by-side fashion. Using both biological fluids and cells from autologous sources, it is possible using this platform to implement very effective and personalized therapies, tailored for the needs of specific patient conditions.

Key Words: Growth Factors, Biological Fluids, Antibodies, Covalent immobilization, Electrospun Nanofibers

3.1 Introduction

The biofunctionalization of surfaces gained special interest by the need to optimize the biological integration of implantable medical devices [1]. Of particular interest is the immobilization of antibodies, due to the high specific interaction with their ligand molecules, making a more efficient and irreversible attachment of the target protein/ligand. Protein immobilization requires that the substrate should provide a biocompatible and bioactive environment, since it should interact positively with the native structure of the proteins and biomolecules [2]. Antibodies were previously immobilized onto different substrates such as solid surfaces [3], microfluidic platforms [4], carboxyl surfaces [5], micro arrays [6], ultra-flat polystyrene surfaces [7] and gold particles [8]. The ultimate goal of the antibodies' immobilization at the substrate surface is to create specific sites for stimulating cell and proteins adhesion [9].

Different immobilization methods and strategies can be implemented to achieve the biofunctionalization of substrates such as physical adsorption, covalent immobilization or antibody-binding proteins [10]. Covalent immobilization is the most reported method, since it leads to a strong and stable attachment. In this method the presence of functional groups is required in both the substrate and the molecule to be immobilized. Due to the use of coupling agents, modifications of the antigen binding site can occur which may cause loss of functionality of the antibodies. Therefore, there is the need to confirm that the biological activity of the corresponding bound antigen was not compromised. With this immobilization method it is also possible to overcome the problems related to the adsorption method, where often occurs deadsorption and antibody denaturation [9,10].

Electrospun nanofiber meshes (NFMs) are very interesting polymeric substrates due to their high specific surface area, their flexibility in surface functionality and their physical fibrous structure mimicking the morphology of the native extracellular matrix of most tissues [11,12]. Other important properties of electrospun NFMs are their high levels of porosity and a pore size smaller than the dimensions of most cells. Those features are of high importance for various applications in Tissue Engineering and Regenerative Medicine, since electrospun NFMs will have selective permeability to soluble factors hindering the permeation of cultured cells [13].

Proteins, especially growth factors (GFs), have an important role in the regulation of a variety of cellular processes, as well as on the coordination of the healing process of different tissues [14]. GFs functions and purposes range from inducing vascularization and angiogenesis

to cell growth, proliferation and differentiation. Therefore, the local or systemic administration of GFs may be a valuable therapeutic approach in the successful treatment of different chronic wounds [15]. Clinically, GF-based strategies are applied in plastic surgery, bone and cartilage lesions, muscle injuries, ulcers and skin regeneration [16]. Particularly, biological fluids such as the Platelet Lysate (PL), that consist of a cocktail of different GFs (e.g. bFGF, VEGF, TGF-β, PDGF-BB, EGF, IGF-I) provide a complex mixture of chemical signals to the cells at the injury site, which is often associated with a non-specific action [17,18].

The leading goal of the herein presented work is to develop a highly biofunctional nanofibrous substrate, taking advantage of the specific and efficient interactions between a specific antibody and its antigen. With this strategy it is possible to selectively immobilize from a pool of highly concentrated GFs present in the PLs, just the ones of interest for the envisioned application (i.e. bFGF, TGF-β1 and VEGF). Furthermore, this biofunctionalization strategy also enables the simultaneous immobilization of multiple antibodies at a time, distributed in a mixed or in a side-by-side fashion over the same nanofibrous substrate enabling designing studies to elucidate the synergistic effect of the combined GFs.

3.2 Materials and Methods

3.2.1 Materials

Polycaprolactone (PCL; Mw = 70 000 – 90 000 determined by GPC), Chloroform, N,N-Dimethylformamide (DMF), hexamethylenediamine (HMD), 1-Ethyl-3-(3-dimethylaminopropyl)carbodiimide (EDC) and hydroxysuccinimide (NHS) were purchased to Sigma Aldrich and use as received. Mouse anti-Human TGF-β1 monoclonal antibody was purchased from PrepoTech Inc. (Rochy Hill, NJ; USA), rabbit anti-Human bFGF oligoclonal antibody (clone 7HCLC), ABfinity recombinant, was purchased from Life Technologies (Carlsbad, CA; USA); and mouse-anti-Human VEGF (JH121) was purchased from Santa Cruz Biotechnology Inc. (Santa Cruz, USA). Regarding the secondary antibodies, both Alexa Fluor ®488 donkey anti-rabbit IgG (H+L) and Alexa Fluor ® 594 goat anti-mouse IgG (H+L) were purchased from Life Technologies (Carlsbad, CA; USA). The growth factors (GFs), namely the recombinant human TGF-β1, recombinant basic-FGF and recombinant human $VEGF_{121}$ were all purchased from PrepoTech Inc. (Rochy Hill, NJ; USA).

3.2.2 Methods

3.2.2.1 Electrospinning of nanofiber meshes

A 17% (w/v) PCL solution was prepared with an organic solvent mixture of Chloroform and DMF in a 7:3 ratio as described elsewhere [19]. The PCL solution was electrospun by applying a voltage of 13.6 kV, a needle tip to ground collector distance of 18 cm and a flow rate of 1mL/h. After the complete processing of 1mL of PCL solution, the nanofiber mesh (NFM) was allowed to dry for 1 day. This processed NFM was cut into samples of 1cm x 1cm for further assays.

3.2.2.2 Ultraviolet-Ozone irradiation and aminolysis

For the activation of the nanofibers surface, an ultraviolet-Ozone (UV-Ozone) cleaner system was used (ProCleaner™ 220, Bioforce Nanoscience). Both sides of the electrospun NFMs were exposed during 4 minutes to UV-Ozone irradiation, as optimized previously. After this surface activation, amine groups (-NH_2) were inserted at the surface of electrospun nanofibers by immersion in a 1 M HMD (Sigma Aldrich) solution during 1h at 37°C. The amount of –NH_2 (2.83 ± 0.11 nmol/cm^2) was determined indirectly by quantifying the amount of free –SH groups according to Ellman's reagent method [20].

3.2.2.3 Antibodies immobilization

3.2.2.3.1 EDC/NHS ratio and concentrations optimization

EDC/NHS reagents were dissolved in 0.1 MES (2-(*N*-morpholino) ethanesulfonic acid) buffer with 0.9% (wt/wt) NaCl, following pH adjustment to 4.7, and mixed for 15 min at RT for antibody activation. Five different EDC/NHS ratios were tested, (i.e. 1:4, 1:2, 1:1, 2:1 and 4:1, and the optimized ratio was further assayed at four different concentrations (10mM EDC + 40 mM NHS, 26 mM EDC + 104 mM NHS, 50 mM EDC + 100 mM NHS and 100 mM EDC + 400 mM NHS). With the optimized reaction conditions, in terms of EDC/NHS ratio and respective concentrations, the final concentration of the linker in the antibody solution was determined for 1%, 5% and 10% concentrations.

3.2.2.3.2 Optimization of Single Antibody Immobilization and Determination of the Standard Curves

Three different antibodies were immobilized (anti-TGF-β1, anti-bFGF and anti-VEGF) at the surface of the activated and functionalized electrospun nanofiber meshes. A wide range of primary antibody concentrations (from 0 μg/mL to 20 μg/mL) was tested to find out the maximum immobilization capacity of the nanofibrous substrate. The electrospun NFMs were incubated with 200 μl of each primary antibody concentration. After overnight incubation at 4 °C, each mesh was washed twice with 300 μl 0.1 M PBS (5 min each time) and a blockage of 3% BSA was performed for 30 minutes at RT. The BSA solution was removed and the secondary antibody (1:200 in PBS) incubated for 1h at RT. In order to determine the degree of immobilization, an indirect method was used to quantify the fluorescence of unbound secondary antibody solution (n=3 samples, read in triplicate). For the TGF-β1 and VEGF antibodies, Alexa Fluor® 594 was used and the reading parameters were the absorption at 590 nm and the emission at 617 nm. In the case of the anti-bFGF, the selected secondary antibody was the Alexa Fluor® 488 and the reading parameters were 495 nm for the adsorption and 519 nm for the emission spectrum. Negative control samples were also prepared, where all antibody immobilization steps were performed with the exception of the primary antibody incubation, which was substituted by PBS.

3.2.2.3.3 Mixed immobilization of two antibodies

The VEGF and bFGF antibodies were mixed in the same PBS solution at the concentrations optimized before, for a final volume of 200 μl per mesh. The antibodies mixture was incubated overnight at 4°C, and then the samples were washed twice with 0.1 M PBS (5 minutes each) and a 3% BSA incubation step for 30 min at RT was performed to block all the non-specific sites. The BSA solution was removed and the secondary antibody Alexa Fluor® 594 (for anti-VEGF) was incubated for 1h at RT. The exceeding secondary antibody solution was collect for further quantification (n=3 samples, read in triplicate), as previously described, and the sample washed twice. The same approach was carried out for the secondary antibody Alexa Fluor® 488 (for anti-bFGF). Both secondary antibodies were prepared in a 1:200 concentration, diluted in PBS. A negative control sample was performed,

without the immobilization of the primary antibodies, although all the other steps were done. All samples were analyzed under laser scanning confocal microscopy.

3.2.2.3.4 Side-by-side immobilization of two antibodies

In order to obtain a substrate with two different antibodies immobilized in a side-by-side design, a compartmental watertight chamber was developed capable of physically divide a single 1cm x 2cm functionalized electrospun NFM into two distinct areas, without allowing the mixture of the different antibodies solutions (**Figure 3.1).** Two different antibody solutions containing (i.e. anti-VEGF and anti-bFGF) were prepared at the concentrations described above and dropped over each area of the functionalized electrospun NFM. All the antibody immobilization steps (washings, BSA blocking and secondary antibody incubation) were performed, as previously described for the single antibody immobilization. The quantification of unbound secondary antibody was also performed and the samples recovered to characterize the spatial distribution of the antibodies by laser scanning confocal microscope.

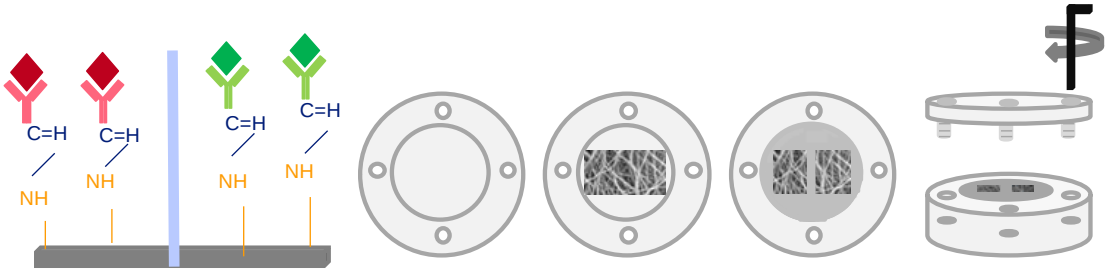

Figure 3.1 Schematic representation of the compartmental watertight device that allows the simultaneous immobilization of two distinct antibodies in two areas of a single mesh.

3.2.2.4 Laser Scanning Confocal Microscopy

Laser Scanning Confocal Microscopy was conducted in order to characterize the spatial distribution of the antibodies at the surface of the electrospun NFMs. The fluorescent labeled biological molecules were analyzed by selecting the appropriate wavelengths: excitation at 495 nm for Alexa Fuor® 488 and 590 nm for Alexa Fluor® 594, and emissions at 570 nm for the red channel and 540 nm for the green channel. The single and multiple (either mixed or side-by-side) antibodies immobilized (i.e. TGF-β1, bFGF and VEGF) samples

were placed onto glass slides and analyzed by laser scanning confocal microcpy (FluoView 1000, Olympus, Germany) at a 10x magnification.

3.2.2.5 Recombinant and PL-derived growth factor quantification

3.2.2.5.1 Platelets Lysates: preparation and activation

Platelet Rich Plasma (PRP) was provided by the "Instituto Português do Sangue", which certifies the biological product accordingly to the Portuguese law. The number of platelets was counted and the sample volume is adjusted to 1 million platelets per μL. At the 3B´s Research Group facilities, the collected PRP samples were subjected to a 3 repeating temperature-shock cycles (i.e. frozen with liquid nitrogen at −196 °C and further heated at 37 °C) and the remaining platelets were eliminated by centrifugation. A pool of Platelet Lysates (PL) was stored at -20°C until further use. At the time of each experiment, a PL solution was thawed and filtered with a 0.22 μm filter.

3.2.2.5.2 Fluorescence-Linked Immunosorbent Assay (FLISA)

After completing all the antibody immobilization steps previously described, 200 μl of the recombinant human protein solutions at different concentrations (ranging from 0 μg/mL to the concentration of each primary antibody) were incubated for 1h at RT. The unbound recombinant human protein solutions were collected and stored at -20°C until further quantification by ELISA. Two 0.1M PBS washing steps (5 minutes each) were performed and the biofunctionalized Nanofibrous substrates were incubated overnight at 4°C with the corresponding primary antibody. After removal of the exceeding primary antibody solutions, the biofunctionalized substrates were washed again with PBS, another BSA blocking step was performed and the corresponding secondary antibody was incubated for 1 hour at RT. The fluorescence of unbound secondary solutions was also read out in a microplate reader (Synergy HT-BioTek). When the PL was used as the natural source of GFs, the same procedure was followed, although the recombinant human protein solution was substituted by 200 μl of PL.

3.2.2.5.3 Enzyme-Linked Immunosorbent Assay (ELISA)

For the unbound GFs quantification, human basic-FGF and VEGF development ELISA kits were purchased from PrepoTech (Rochy Hill, NJ; USA), whereas the human TGF-β1 ELISA kit was brought from Boster Biological Technology (Fremont, Ca; USA). For the bFGF and VEGF development ELISA kits, the primary antibodies were firstly incubated overnight in a 96-well plate (Nunc-Immuno™ MicroWell™ 96 well solid plates, Sigma Aldrich). All solutions were prepared according to the manufacturer protocol and, in the last step, 100 µl of an 2,2'-azino-bis(3-ethylbenzthiazoline-6-sulphonic acid (ABTS) liquid substrate was added to each sample and each plate read at 405 nm and 650 nm, respectively. The TGF-β1 ELISA is a ready-to-use kit, where the bottom wells were previously coated with the antibody. Both the standards and the samples were incubated and the assay conducted according to the protocol of the manufacturer protocol. In the last step of the procedure, 100 µl of the 3,3′,5,5′-Tetramethylbenzidine (TMB) stop solution was added to each well and the absorbance at 450 nm was read out (Synergy HT, Bio-TEK).

3.2.2.6 Biological Assays

3.2.2.6.1 Cell culture and seeding

A human pulmonary microvascular endothelial cell line (HPMEC-ST1.6R) was used to validate the developed biofunctionalized nanofibrous substrate. This cell line is used to study *in vitro* angiogenic process [21].

HPMEC-ST1.6R cells were cultured with M199 medium (Sigma Aldrich) supplemented with 20% FBS (Alfagene), 2 mM Glutamax (Life Technologies), Pen/Strep (100 U/100 g/mL; Life Technologies), heparin (50 µg/mL; Sigma Aldrich), Endothelial cell growth supplement (ECGS - 25 µg/mL; Becton Dickinson) and incubated at 37°C in a humidified 5% CO_2 atmosphere. HPMEC-ST1.6R cells were used at passages 30-32. Medium was changed twice a week until cell reached 90% of confluence. Then, cells were harvested and seeded onto the activated and functionalized electrospun NFMs.

The electrospun PCL NFMs were sterilized by ethylene oxide at Pronefro® Produtos Nefrológicos, S.A. (Porto, Portugal). For NFM_AB1, NFM_Ab2, NFM-$VEGF_{Rec}$ and NFM+$VEGF_{PL}$, VEGF antibody was immobilized overnight and, after the BSA blocking step, human recombinant protein (VEGF=4 µg/mL) and PL were incubated. Cell seeding was

performed by dropping a 50 µl cell suspension containing 50 000 cells per substrate and left overnight. After cell attachment, culture medium was added to each type of cells and conditions. Untreated electrospun PCL NFMs (NFM) and NFMs where nanofibers were subjected to surface activation, aminolysis and primary antibody immobilization (NFM_Ab1) were used as controls. After 1, 3 and 7 days of culture, samples were collected for cell viability assay, DNA and total protein quantification and VEGF quantification.

3.2.2.6.2 Cell Viability

The metabolic activity of HPMEC-ST1.6R cells seeded on untreated electrospun PCL NFM, NFMs with primary antibody immobilization, and biofunctionalized nanofibrous substrates (recombinant and PL-derived) was determined by the MTS assay (CellTiter 96 ® AQ_{ueous} One Solution, Promega). At days 1, 3 and 7, the culture medium was removed and the samples were rinsed with sterile PBS. A mixture of culture medium and MTS reagent (5:1 ratio) was added to each mesh, as well as to the negative control comprising no cells or samples. All conditions were performed in triplicate and left to incubate for 3h, at 37 °C in a humidified 5% CO_2 atmosphere. Thereafter, the absorbance of the MTS reaction medium from each sample was read in triplicate at 490 nm (Synergy HT, Bio-TEK).

3.2.2.6.3 Cell proliferation

Cell proliferation was determined by using a fluorimetric dsDNA quantification kit (Quant-iT™, PicoGreen®, Molecular Probes, Invitrogen, USA). The samples were collected at days 1, 3 and 7, washed twice with sterile PBS and transferred into eppendorf tubes containing 1 mL of ultrapure water. These samples were frozen at -80 °C until further analysis. Prior to DNA quantification, the various specimens for each samples were thawed and sonicated for 15 min. DNA standards were prepared at concentrations ranging from 0 to 2 µg/mL. Per each well of an opaque 96-wells plate (Falcon) were added 28.7 µL of sample or standard (n=3), 71.3 µL of PicoGreen solution and 100 µL of TE buffer. The plate was incubated for 10 min in the dark and the fluorescence was measured in a microplate reader (Synergie HT, Bio-Tek; USA) by using an excitation wavelength of 480 nm and an emission

wavelength of 528 nm. The DNA concentration of each sample was calculated using a standard curve relating DNA concentration and fluorescence intensity.

3.2.2.6.4 Total Protein synthesis

Samples were collected and prepared for assaying, as previously described in the Cell Proliferation. For the quantification of total protein synthesis, a Micro BCA™ Protein Assay Kit (Pierce, Thermo Scientific) was used. The assay was made accordingly to the manufacturer instructions. Briefly, standards were prepared at various concentrations ranging from 0 μg/mL to 40 μg/mL in ultra pure water. 150 μL of both samples and standards were assayed in triplicate and 150 μl of working reagent were further added to each 96-well plate. The plate was sealed and incubated for 2 hours at 37 °C. The plate was left to cool down to RT and, thereafter, the absorbance at 562 nm was measured in a microplate reader (Synergy HT, Bio-Tek).

3.2.2.6.5 Statistical analysis

Statistical analysis was performed using Graph Pad Prism Software. Differences between the different conditions of the cellular assays were analyzed using non-parametric test (Kruskal-Wallis test) and a $p<0.05$ was considered significant. Data were presented as mean ± standard deviations.

3.3 Results and Discussion

The first task of this work was to activate and functionalize the surface of electrospun PCL nanofibrous meshes to allow the binding of specific growth factors from a pool of different proteins. In this experiment the biological fluid used in the tests was platelet lysate (PL). To achieve that selective binding, specific antibodies were immobilized at the nanofibrous substrate surface assuring that only the growth factors of interest is immobilized. The covalent immobilization was the preferred methodology to immobilize the antibodies at the surface of the chemically modified electrospun PCL nanofiber meshes (NFMs). We

herein used carboxyl groups and amines as they tend to react leading to an efficient covalent immobilization [10,22]. Particularly, there is a carboxyl group (-COOH) at the end of the non-variable region of the antibodies that react with the amine groups (-NH_2) that were previously inserted at the surface of electrospun nanofibers, leading to the covalent immobilization of an antibody to the polymeric substrate. In this immobilization procedure some steps were optimized such as the coupling agent EDC/NHS ratio and concentrations, the maximum immobilization capacity of the activated and functionalized electrospun nanofibers, and the GFs binding capacity of the nanofibrous substrate. An endothelial cell line was used as a living model to assess the bioactivity of bound VEGF. The successful single antibody immobilization strategy was then transposed to different spatial configurations, by the immobilization of two antibodies (i.e. anti-bFGF and anti-VEGF) in the same nanofibrous substrate, in a mixed or in a side-by-side fashion.

From the most reported biomolecules present in PL (i.e. TGF-β1, PDGF-ββ, bFGF, EGF, IGF, and VEGF) [17,23] TGF-β1, bFGF and VEGF were selected to conduct our validation experiments. TGF-β1 has an important role in promoting the production of ECM and in enhancing the proliferation of both fibroblasts and osteoblasts, being therefore relevant for both bone and cartilage strategies [24–26]. bFGF is a potent inductor of cell proliferation, promoting angiogenesis and differentiation, as well as collagen production. It has a significant function in bone, cartilage and periodontal tissues [27–29]. VEGF is a promoter of angiogenesis and proliferation of endothelial cells, playing a pivotal role in vascularization and stem cell differentiation [30–32].

3.3.1 Optimization of Antibodies Immobilization

3.3.1.1 EDC/NHS ratio and concentrations

In the present study, a defined antibody was immobilized at the surface of electrospun nanofibers by a covalent bound mediated by a coupling agent, in this particular case the EDC/NHS mixture. Prior to the immobilization step, the electrospun PCL NFMs needed to be chemically modified by the insertion of amine groups that could react specifically with the carboxyl groups of the antibody [19]. It is know that EDC alone is able to increase the immobilization efficiency of biomolecules [9,33]. However, with the addition of NHS, a two-step reaction occurred and the presence of NHS forms semi-stable amines, enhancing the

immobilization efficiency of the antibodies at the surface of a substrate [34]. In order to ensure that the nanofibrous substrate is being used at its maximum immobilization capacity, different parameters concerning these two coupling reagents were tested.

The first parameter assessed was the ratio between the EDC/NHS coupling agents. Different ratios were tested (**Figure 3.2 a)**) and the 1:4 ratio present the highest immobilization efficiency and lower variability being therefore selected for further experiments. Looking at the different ratios it seems that higher concentrations of NHS lead to a higher efficiency of immobilization. With the selected ratio, the next step was to optimize the concentration of each individual coupling agent (**Figure 3.2 b**)). From the four concentrations tested, the one that yields less variability and higher efficiency was the 50 mM EDC + 200 mM NHS and, therefore, the one selected for further experiments. The final step of this optimization process relies on testing the concentration of the EDC/NHS mixture in the final antibody solution. The EDC/NHS concentration that got higher immobilization efficiency was the 1% (v/v), since the amount of immobilized antibody decreases with the increase of EDC/NHS concentration (**Figure 3.2 c)**). Based on these results, all further experiments concerning antibodies immobilization will use the following optimized conditions: 1:4 ratio, 50mM EDC + 200 mM NHS concentrations and 1% (v/v) EDC/NHS concentration in the primary antibody solution.

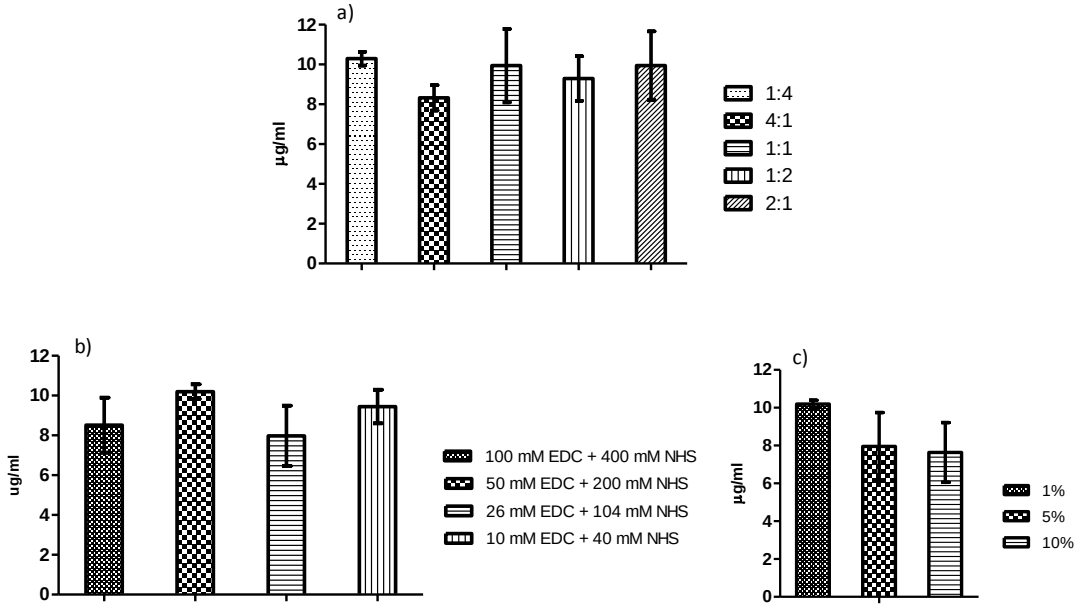

Figure 3.2 EDC/NHS ratio and concentrations optimization. (a) optimization of the coupling agents EDC/NHS ratio; (b) optimization of the individual EDC and NHS concentrations, maintaining the previously optimized ratio 1:4; (c) optimization of the final concentration of the EDC/NHS mixture (50 mM EDC + 200 mM NHS, optimized before) in the antibody solution.

3.3.2 Single antibody immobilization at the Nanofibrous surface

3.3.2.1 Antibodies immobilization efficiency

The antibodies against the growth factors TGF-β1, bFGF and VEGF were immobilized at the surface of activated and functionalized electrospun nanofibers, in a wide range of concentrations (0 – 20 μg/mL), to determine the maximum immobilization capacity of the nanofibrous substrate for each antibody. To achieve that purpose, an indirect quantification method was used, based on the measurement of unbound secondary antibody fluorescence, after its incubation with the immobilized primary antibody. As observed in **Figure 3.3**, the higher amount of immobilized primary antibody corresponds to the lower fluorescence signal of the free secondary antibody. When the fluorescence signal reaches a plateau, the nanofibrous substrate presents the maximum concentration of immobilized primary antibody, reaching the saturation of the system. With the anti-TGF-β1, the maximum concentration of immobilized primary antibody is 12 μg/mL; in the case of anti-bFGF, the maximum capacity of the nanofibrous substrate is 8 μg/mL; whereas with the anti-VEGF its concentration reaches a value of 4 μg/mL. As clearly noticed, the different antibodies have different densities over the same activated and functionalized nanofibrous substrate. This observation may be related with the different sizes of the primary antibodies used. According to manufacturer's data the size of anti-VEGF is approximately 22 kDa and anti-bFGF is 17 kDA. In the case of the anti-TGF-β1 no information is given by the company although according to other manufacturers, the molecular weight of anti-TGF-β1 should be around 12-14 kDA. The immobilization data correlates with the antibodies size, since the more surface area is occupied by the antibody, the lower is its concentration at the nanofibers surface. Therefore, further experiments were performed with the concentrations of the primary antibodies that lead to the maximum immobilization capacity of the nanofibrous substrate. Antibodies were immobilized in different subtracts as referred before in a similar fashion as the common ELISA methods, that also involve the immobilization of specific antibodies at the bottom of the well to quantify the amount of specific antigen existing in a sample. From the datasheet of the ELISAs, referred in the materials and methods section, it is possible to conclude that the values for anti-bFGF and anti-VEGF immobilization is 1 μg/mL and 0.5 μg/mL, respectively. The ELISA tests are conducted in 96 well-plates having approximately 0.32 cm^2 of surface area per well. In the case of the developed biofunctionalized nanofibrous substrate

the apparent surface area is about three times higher (1cm²) and despite having the same ratio between them the immobilization capacity is 8 times (8 μg/mL for anti-bFGF and 4 μg/mL for anti-VEGF)higher than in the standard ELISAs.

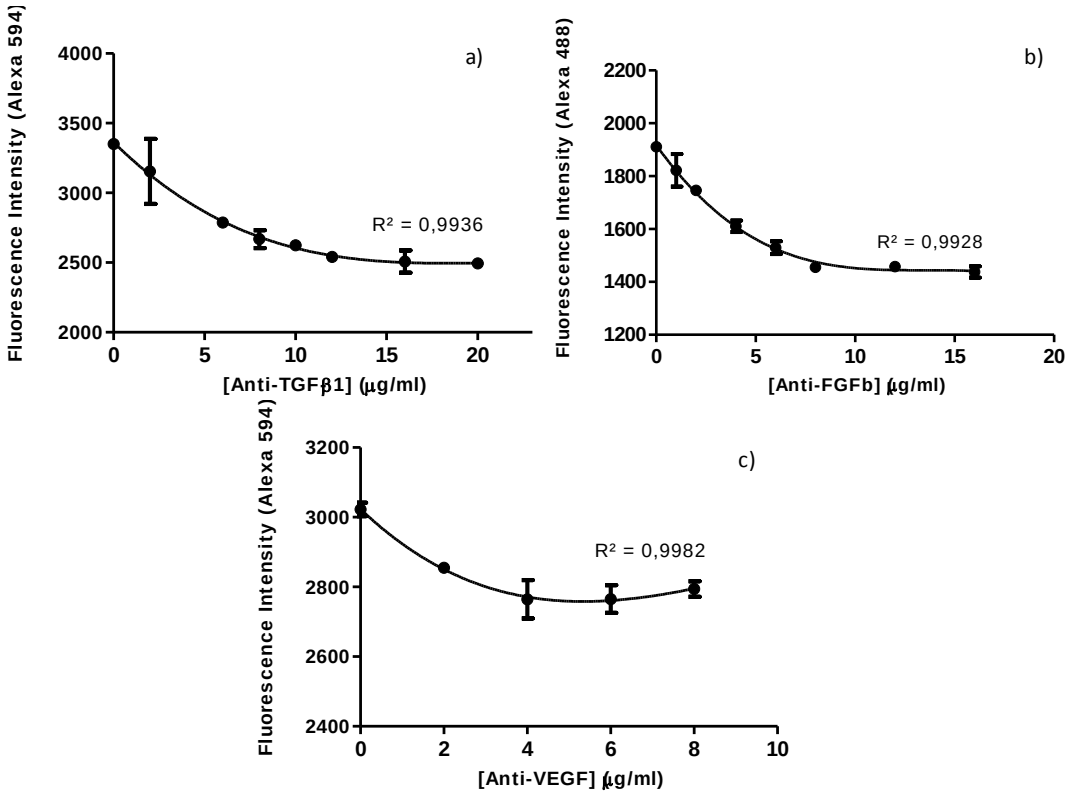

Figure 3.3 Maximum immobilization capacity of a single antibody at the surface of activated and functionalized electrospun nanofiber: a) immobilization of anti-TGF-β1, b) immobilization of anti- bFGF and c) immobilization of anti-VEGF.

3.3.2.3 Primary antibodies standard curve

After determining the maximum antibody concentration immobilized at the surface of the activated and functionalized electrospun nanofibers, a standard curve was determined for each antibody. With the remaining solution of each secondary antibody, it was possible to determine the amount of unbound secondary antibody, leading indirectly to the concentration of primary antibody that was immobilized. A linear regression standard curve fitting those data points allowed obtaining a R^2 above 0.98 for every antibody (**Figure 3.4**). These standard curves were further used for the quantification of the immobilized antibodies in next assays.

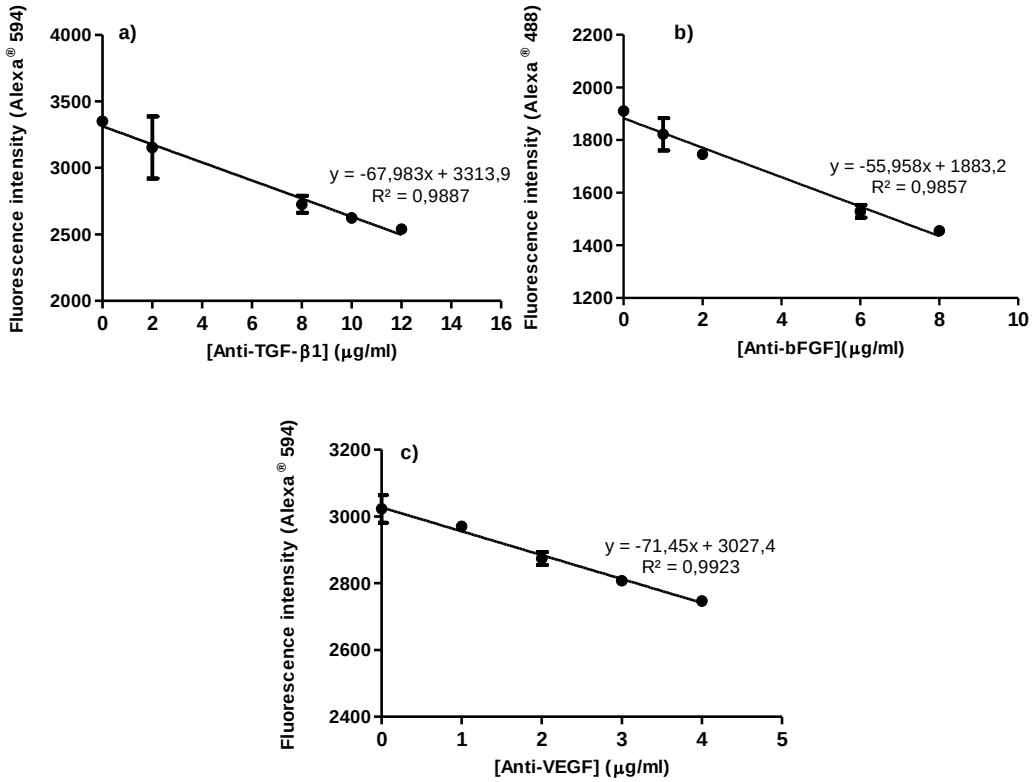

Figure 3.4 Standard curves for single antibody immobilization at the surface of activated and functionalized electrospun nanofibers. a) TGF-β1 antibody standard curve varying between 0 μg/mL and the maximum concentration that can be immobilized (i.e. 12 μg/ml). b) bFGF antibody standard curve ranges from 0 μg/mL to 8 μg/mL; and c) VEGF antibody standard curve varies between 0 μg/mL and 4 μg/mL.

3.3.2.2 Spatial distribution of antibodies at the surface of electrospun nanofibers

The spatial distribution of the TGF-β1, bFGF and VEGF antibodies at the surface of activated and functionalized electrospun nanofibers is shown in **Figure 3.5**. All the immobilized antibodies seem to be uniformly distributed through the nanofibers surface, resembling the random mesh-like arrangement of the electrospun NFM structure. The TGF-β1 antibody seems to have a more intense and densely distributed fluorescence than the other immobilized antibodies, probably due to its higher concentration (12 μg/mL). To ensure that the secondary antibody only binds to the immobilized primary antibody, we defined a control experiment in which all the steps were performed except the incubation with the primary antibody. These conditions were analyzed for fluorescence (**Figure 3.5 d),**

e) and f)) and no fluorescence was detected. Since no fluorescent signal was observed , it means that Alexa Fluor ®594 and Alexa Fluor ® 488 secondary antibodies were not immobilized at the surface of activated and functionalized electrospun nanofibers, confirming the specific binding between these two secondary antibodies and the corresponding immobilized primary antibodies.

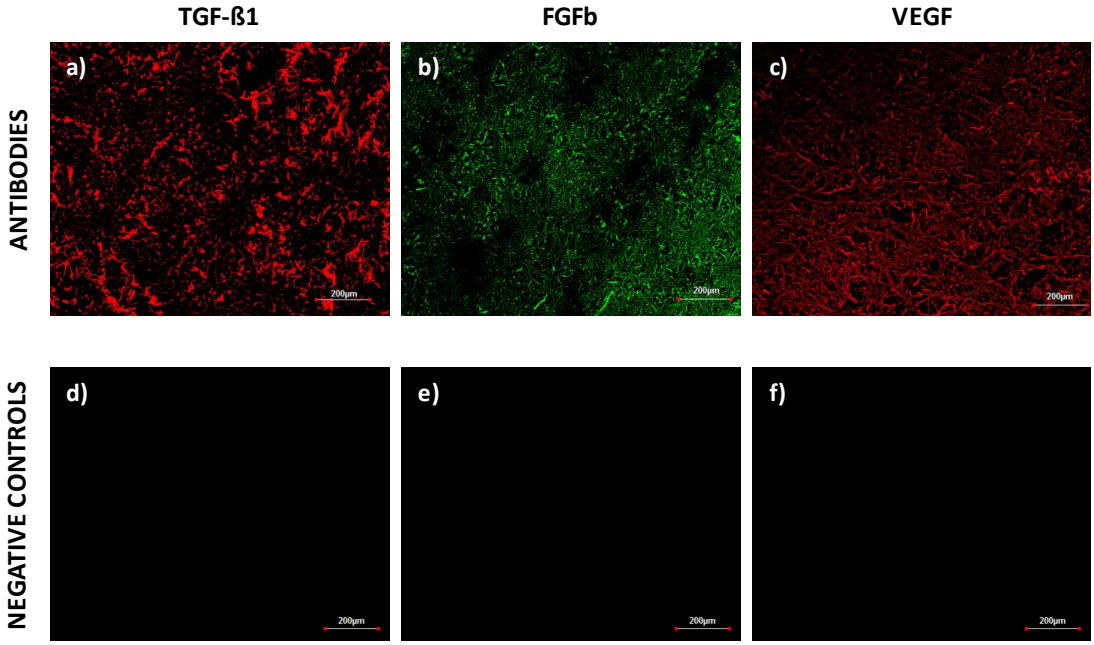

Figure 3.5 Spatial distribution of immobilized primary antibodies at the surface of activated and functionalized electrospun nanofibers. Primary antibodies were immobilized at the previous optimized concentrations: a) 12 µg/mL of anti-TGF-β1, b) 8 µg/mL of anti-bFGF and c) 4 µg/mL of anti-VEGF. In the case of the TGF-β1 and VEGF antibodies, the secondary antibody Alexa Fluor ® 594 was used, whereas the secondary antibody Alexa Fluor® 488 was used for the bFGF antibody. The negative controls d), e) and f) were subjected to all the steps except the incubation with the primary antibodies.

3.3.3 Growth Factors binding capacity to the biofunctionalized nanofibrous substrate

3.3.3.1 Quantification of bound recombinant proteins

After confirming the specific immobilization of the TGF-β1, bFGF and VEGF antibodies and determining the corresponding standard curves, it was assessed the binding capacity of the biofunctionalized nanofibrous substrates. Namely it was characterized the total amount of each growth factor that a functionalized mesh can bind. For that, two different growth factor (GF) sources were tested: (i) recombinant proteins to evaluate the maximum binding capacity

of the biofunctionalized nanofibrous substrate, and (ii) PL-derived GFs to assess the selective binding capacity of the biofunctionalized nanofibrous substrate. In fact, when using recombinant protein, we know that the only protein competing to the primary antibody is the one being tested. In PLs we have a complex mixture of proteins competing for the antibodies, thus demonstrating the specificity of the bound proteins.

Following the immobilization of each antibody at the surface of the activated and functionalized electrospun nanofibers, the corresponding recombinant protein was added at different concentrations, varying from 0 μg/mL to values higher than the concentration of the previously immobilized primary antibody. However, for all the three antibodies in study, the biofunctionalized nanofibrous substrate starts to reach its maximum GF binding capacity near to the higher concentration of the primary antibody as showed in **Figure 3.6** (i.e. 12 μg/mL for TGF-β1, 8 μg/mL for bFGF and 4 μg/mL for VEGF). The results were also confirmed and quantified with commercial available ELISA and the maximum loading capacity corresponded to the above mentioned values, reaching around 100% of loading efficiency for all the three GFs. As observed in **Figure 3.6**, an increase in the amount of recombinant protein leads to a decrease in the fluorescence signal, meaning that less secondary antibodies are unbound. It is important to notice that each GF-bound to the biofunctionalized nanofibrous substrate has its own slope or rate. The higher slope is observed for TGF-β1 (40,833), followed by the one for bFGF (27,259) and the lower one for VEGF (21,771). The possible explanation for this observation relies on the fact that higher concentrations of primary antibodies are occupied faster by the corresponding recombinant protein, leading to a rapid decrease on the fluorescence signal of the unbound secondary antibody. TGF-β1 has been previously reported to be immobilized in different substrates like gelatin [35] and magnetic beads [36] whereas bFGF has been immobilized into different platforms like, PEG hydrogel [37], PLGA films [38] and PLLA+collagen scaffolds [39]. VEGF has been covalently immobilized into different substrates such as collagen scaffolds [40,41], PLGA [42] and hydrogels [43]. From all this literature data, it was possible to conclude that our nanofibrous substrate enables immobilizing a higher concentration of GFs at the order of μg/mL, whereas most of the other system reported values that are at the magnitude of ng/mL, reflecting the positive effect of the increased surface area of the electrospun nanofibers over the bound GFs.

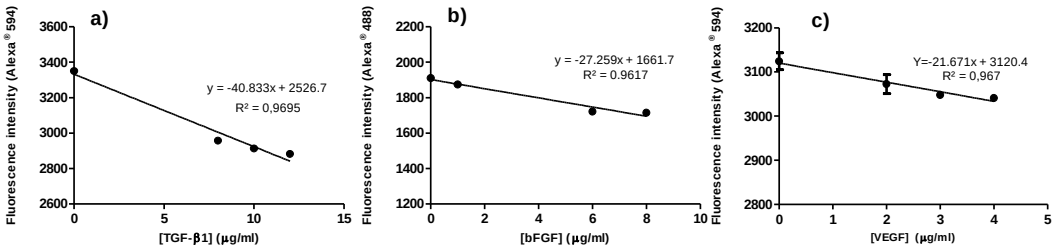

Figure 3.6 Capability of the biofunctionalized nanofibrous substrate to bind different concentrations of the recombinant protein: a) TGF-β1, b) bFGF and c) VEGF.

3.3.3.2 Quantification of bound PL-derived growth factors

We quantified the amount of each GF of interest in the PL by an ELISA kit. **Table 3.1** shows the range of concentrations obtained from two different human samples. Comparing to other values reported in the literature, TGF-β1(169.9±84.5 ng/mL) is about 15 times higher than the ones obtained with our own samples whereas the values of VEGF are comprised in the reported values (0.076 to 0.854 µg/mL)[17]. Despite being described as one of the most abundant GFs of PRP samples, we found no data reporting the concentration of bFGF in the literature. The differences of the quantified GFs and its variability are related with the differences between donors leading to different concentrations of the GFs of interest.

Table 3.1 Quantification of the growth factors of interest derived from two human PL samples

Growth Factors	Concentration in PL samples		% Binding	
	Donor 1	Donor 2	Donor 1	Donor 2
TGF-β1	4.2 ng/mL	11.05 ng/mL	83.92 ± 2.68	86.85 ± 3.26
bFGF	8.6 ng/mL	102.5 ng/mL	54.78 ± 4.75	63.97 ± 3.48
VEGF	0.0949 ng/mL	0.4263 ng/mL	49.52 ± 3.05	58.85 ±4.02

After determining the recombinant human GF binding capacity of the activated and functionalized nanofibrous substrate, it was tested for the selective binding of GFs derived from the PL samples. ELISAs were performed to determine the amount of bound autologous

GFs for two different donors. For PL-derived TGF-β1, the binding efficiency (around between 84% - 87%) was not as high as in the case of the recombinant protein. Considering the bFGF, only around 55% - 64% of PL-derived protein was bound to the nanofibrous substrate immobilized primary antibody. The same trend was observed for the VEGF, where about 50% -58% of PL-derived VEFG was bound by the corresponding immobilized antibody. Despite the concentrations of the GFS in the different samples the bounding of the GFs stayed in the same range for the two donor samples, showing the consistency of the method.

Despite the order of magnitude differences in the concentration of GFs present in the PL (ranging from pg/mL for VEGF to ng/mL for TGF-β1 and bFGF), those concentrations are much lower than the ones determined for the maximum binding capacity of the biofunctionalized nanofibrous substrate where recombinant proteins were used at μg/mL. The inability of the biofunctionalized nanofibrous substrate to immobilize 100% of the GFs amount present in the PL can be related with the fact that this biological fluid is highly rich in different GFs and proteins that can compete to the binding sites of each immobilized antibody. Another technical aspect that can justify the binding of GFs derived from the PL in the range of 50-87% is the detection limits of the used ELISAs, which do not enable detecting the GFs at very low concentrations (16 pg/mL for VEGF ELISA Kits, 63 pg/mL for bFGF and 15.6 pg/mL for TGF-β1).

3.3.4 VEGF biological activity

To confirm that the covalent immobilization method do not compromise the bioavailability of the antigen binding site of the antibodies and the behavior of the bound growth factors we assessed the bioactivity of bound VEGF. VEGF has been described to induce vascularization and angiogenesis so human pulmonary microvascular endothelial cells (HPMEC-ST1.6R cell line) were seeded onto the biofunctionalized electrospun nanofibrous substrates. VEGF condition was selected since VEGF is less concentrated factor in Platelet Lysate so we assessed the bioactivity for the worst (less concentrated) scenario. Different biological assays were conducted to assess the endothelial cells viability and proliferation, the total protein synthesis, as well as the quantification of intracellular synthesis of VEGF (**Figure 3.7**). The endothelial cells were cultured at the surface of 5 different substrate conditions : i) untreated electrospun PCL NFM (NFM), ii) NFM with primary antibody (NFM_Ab1), iii)

electrospun NFM with bound recombinant VEGF (NFM+$VEGF_{Rec}$), iv) electrospun NFM with PL-derived VEGF (NFM+$VEGF_{PL}$) and v) NFM with primary anti-VEGF (NFM_Ab2). In conditions i) and ii) the medium was supplemented with Endothelial Cell Growth Supplement (ECGS), a mixture of growth factors aimed to stimulate the growth of human and animal vascular endothelial cells [44,45]. In conditions iii), iv) and v) the endothelial cells were cultured in basal medium since we wanted to evaluate the actions of the immobilized form of VEGF so the medium was not supplemented by other GFs.

Our data confirms the biological activity of the bound VEGF, since in all the assays performed (cell proliferation, cell viability, total protein synthesis and intracellular VEGF), we always report significant differences between the NFM+$VEGF_{Rec}$ and NFM+$VEGF_{PL}$ when compared to NFM_Ab2 (this condition only differs from the previous one by not having an immobilized protein). This observation undoubtedly demonstrates that bound VEGF (recombinant or PL-derived) indeed make a difference in the biofunctionalized nanofibrous substrate. Furthermore, no significant differences were observed at first day, regarding the cell DNA content (**Figure 3.7 a)**), confirming the similar number of cells seeded over the different substrate. Since there are no significant differences between NFM+$VEGF_{PL}$ and NFM+$VEGF_{Rec}$ even at a much higher concentration of recombinant VEGF (4 μg/mL) it is possible to conclude that the amount of protein derived from PL samples (0.251 μg/mL) is enough to induce cells proliferation. Although an excess of immobilized recombinant protein did not have adverse effects on the endothelial cells. Our controls do not present significant differences among them showing that the chemical treatment do not affect cells behavior. Another important aspect of those cellular experiments is the observation of significant differences between the bound VEGF and the conditions where the GFs are given in its soluble form (NFM and NFM_Ab1) demonstrating its bioactivity along time. This same trend has already been reported showing some evidences that the immobilized form can be beneficial for endothelial cells metabolic activity and protein synthesis [40]. This is probable due to the fact that immobilized VEGF can provide a more controlled and sustained influence over the cells, comparing with the transient effect of soluble VEGF. GFs immobilization in substrates also promotes a local regulation and control over cellular activity, as expressed by the intracellular VEGF over expression. Furthermore, immobilized growth factors can provide extended signaling since the ligant will not be internalized as a ligant/receptor complex.

Covalent attachment of angiogenic growth factors to biomaterial scaffolds is a advantageous strategy for the development of polymeric matrix with enhanced angiogenic capabilities.[46]

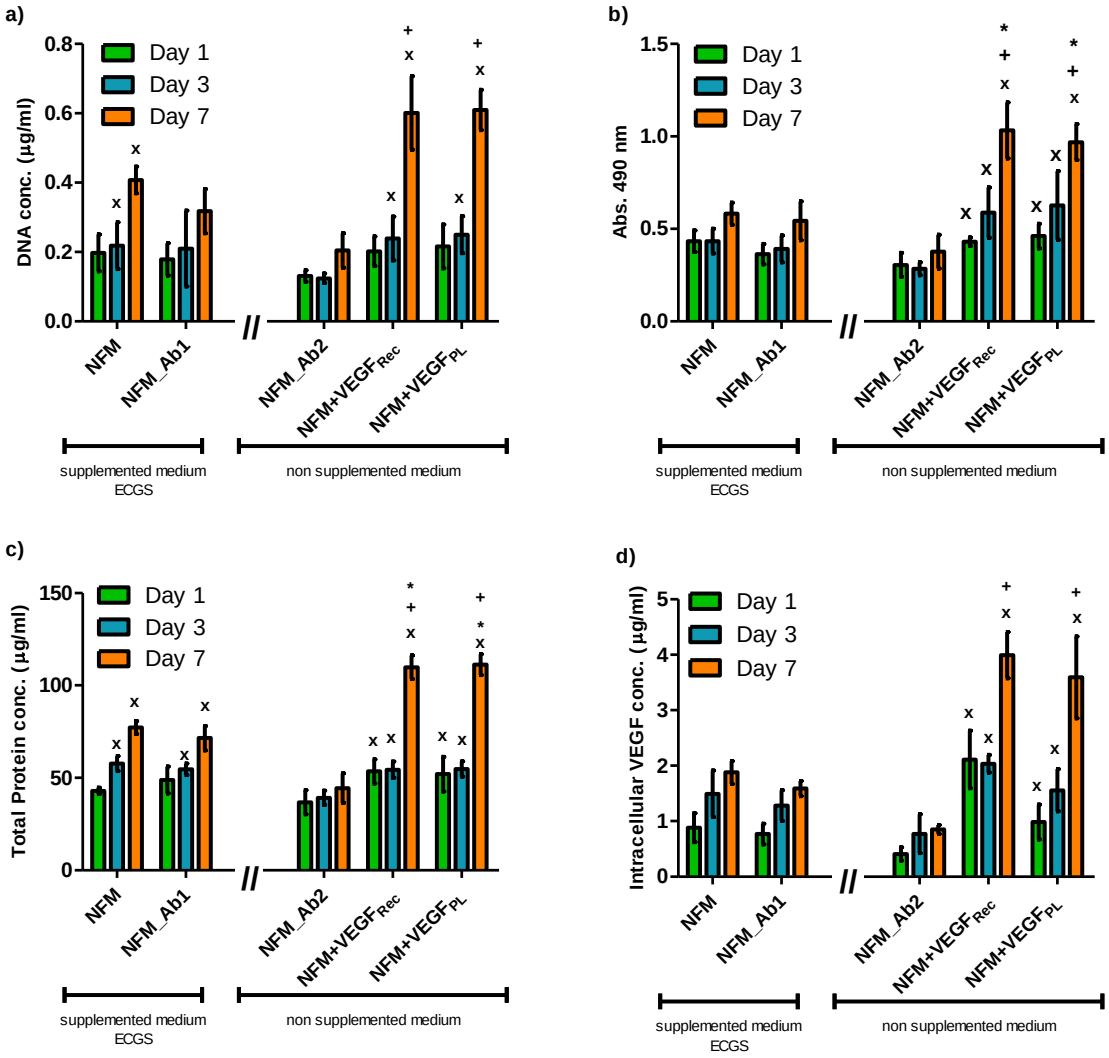

Figure 3.7 Biochemical performance of the endothelial cell line cultured on unmodified electrospun PCL NFM, NFM with immobilized VEGF antibody (NFM_Ab1), both in supplemented medium (ECGS); NFM with immobilized VEGF antibody (NFM_Ab2), NFM with bound recombinant VEGF (NFM+$VEGF_{Rec}$) PL-derived VEGF (NFM+$VEGF_{PL}$) with non supplemented media a) Cell Proliferation, b) cell viability, c) total protein synthesis and d) intracellular VEGF synthesis. Statistical analysis was performed for the five different conditions comparing each time point (Day 1, Day 3 and day 7). Data was considered statistical different for p values < 0.05. (*****) denote significant differences when compared to NFM condition, (+) when compared to NFM_Ab1 supplemented media, (x) when compared to NFM_Ab2, (#) when compared to NFM_VEGF and (&) when compared to NFM_PL.

3.3.5 Immobilization of multiple antibodies in different spatial configurations

Our methodology herein reported aims at immobilizing more than one antibody at the surface of a single activated and functionalized NFM. Two different immobilization designs will be presented: one with the mixed distribution of defined antibodies (i.e. anti-VEGF and anti-bFGF) and another with side-by side localization of those distinct antibodies, in different areas of the same nanofibrous substrate. With the immobilization of multiple antibodies at the surface of the same nanofibrous substrate it is expected to develop a highly efficient system for designing advances strategies for diverse cell biology, tissue engineering and regenerative medicine.

3.3.5.1 Mixed immobilization of two different GFs

The purpose of the mixed immobilization is to have, at the surface of the same nanofibrous substrate, two different but complementary antibodies, specifically the anti-bFGF and anti-VEGF. To implement this strategy, the antibodies concentrations optimized before (i.e. 8 μg/mL for bFGF and 4 μg/mL for TGF-β1) were used and incubated simultaneously.

The **Figure 3.8 a)** express how much of the initial antibodies concentrations have been immobilized, being these results obtained by applying the determined standard curves for the single antibody immobilization strategy (**Figure 3.4**). In the case of anti-bFGF, around 63% of the initial antibody concentration was immobilized, whereas around 72% of the initial concentration was immobilized in the case of VEGF antibody. These immobilization efficiencies were above the expected outcomes, since the two antibodies, although at different concentrations, are competing for the same amount of NH2 available at the surface of an activated and functionalized nanofibrous substrate. The antibodies can be immobilized until the system reaches its maximum capacity, not having more chemical groups available for the antibodies immobilization. Therefore, in the mixed distribution of two antibodies is reasonable that the immobilization efficiency could not be as high as for the single immobilization strategy. Human PL samples were also incubated with the mixed immobilization nanofibrous substrate to evaluate if this system was able to bind selectively and simultaneously the two growth factors of interest. As observed in **Figure 3.8 b)**, the binding efficiency was about 64% for bFGF and 65% for VEGF.

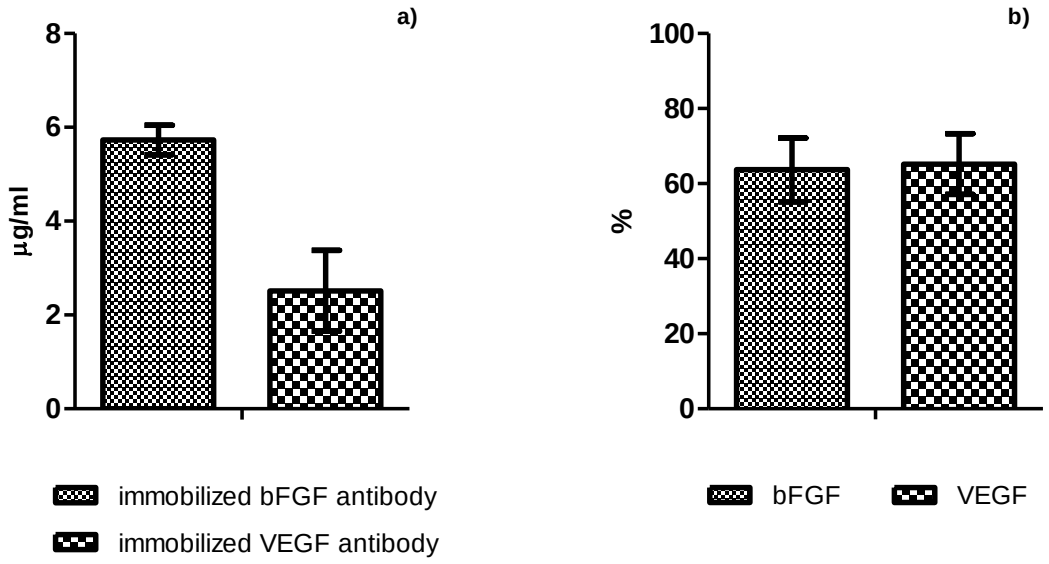

Figure 3.8 (a) Quantification of mixed immobilized bFGF and VEGF antibodies. (b) relative quantification of bound GFs (i.e. VEGF and bFGF) derived from PL.

To evaluate the spatial distribution and confirm that both antibodies were indeed immobilized at the same nanofibrous substrate in a mixed design, the corresponding secondary antibodies were used and their fluorescence observed at the laser scanning confocal microscope.

Figures **3.9 a) and b)** represent the Alexa Fluor ®488 and the Alexa Fluor ®594 fluorescent antibodies bound to the anti-bFGF and anti-VEGF at the surface of activated and functionalized nanofibrous substrate. It is possible to observe that the antibodies are uniformly distributed over the functionalized nanofibrous substrate. However, it is also possible to notice that the green fluorescence is slightly more intense than the one concerning anti-VEGF immobilization. This may be related with the higher concentration of the immobilized anti-bFGF, which can lead to higher intensity of Alexa Fluor ® 488 antibody fluorescence. **Figure 3.9 c)** represent the merge of the two different channels/fluorescences (green and red), corresponding to the VEGF and bFGF immobilized antibodies distribution. The merging of the two pictures yield a significant amount of yellow spots which demonstrate the co-localization of both antibodies in a mixed fashion, over the same nanofibrous substrate. Finally **Figure 3.9 d**) presents the negative control of the experience, where the incubation step with the primary antibodies solution was not conducted to make sure that the secondary antibodies are only bind to the corresponding primary antibodies.

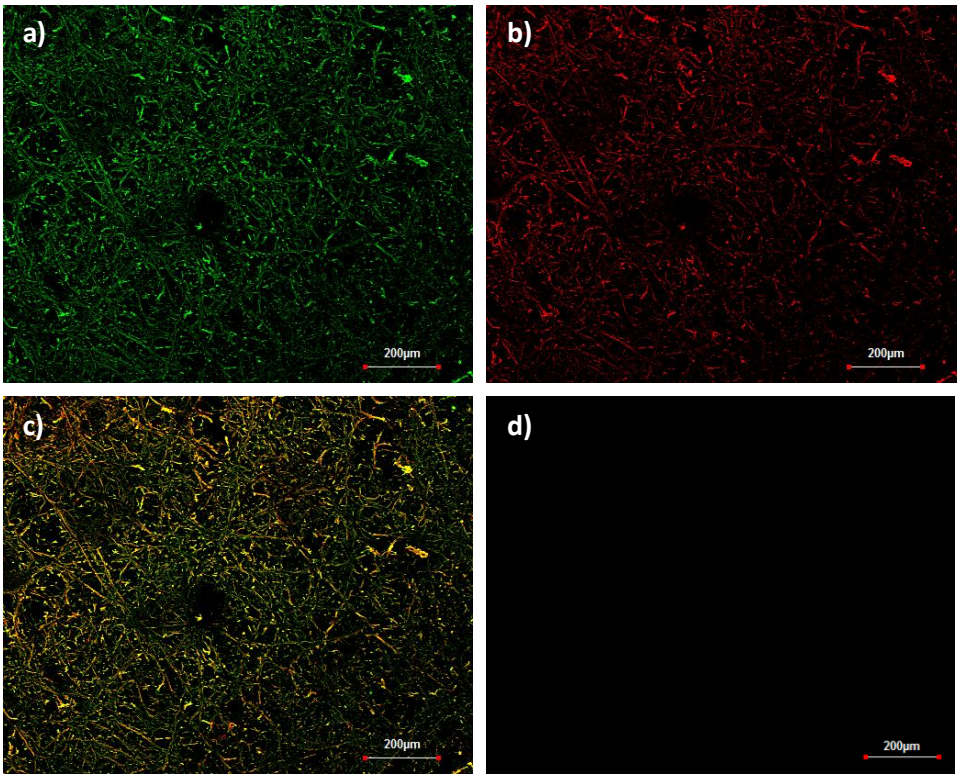

Figure 3.9 Spatial distribution of the mixed immobilized primary antibodies at the surface of a single activated and functionalized Nanofibrous substrates. The bFGF and VEGF antibodies were simultaneously immobilized in the same mesh, at the previously optimized concentrations. a) Alexa Fluor ® 448 was used as the secondary antibody for the anti-bFGF); b) the Alexa Fluor ® 594 was used for the anti-VEGF; c) the spatial distribution of the two primary antibodies (merge view); and d) activated and functionalized Nanofibrous substrates without primary antibodies immobilization.

3.3.5.2 Side-by-side immobilization of two distinct antibodies

With the side-by-side immobilization of two antibodies we intend to demonstrate the possibility to have two distinct GFs selectively immobilized from biological fluids, bound side by side, having in mind their functional role over two distinct cell types spatially juxtaposed in physiological environments. In order to achieve this purpose, a compartmental watertight device was designed to enable creating two distinct areas in the same nanofibrous substrate. Each area of the activated and functionalized nanofibrous substrate was incubated with the defined primary antibody and, further with the corresponding secondary antibody, leading to the side-by-side configuration and distribution presented in **Figure 3.10**. The reddish fluorescent area of the nanofibrous substrate corresponds to the anti-VEGF immobilization,

whereas the green area reports to the bFGF antibody immobilization. The black area corresponds to the bar that separates the same nanofibrous substrate into the two areas. It is possible to detect local green spots or red dots which can be due to some diffusion of the antibodies solution trough the activated and functionalized nanofibrous substrate.

With this system it will be possible to seed and culture two different cell types over the two areas of the biofunctionalized nanofibrous substrate, where defined antibodies and the corresponding GFs are previously immobilized. With this strategy it will be possible to obtain tailored and advanced co-culture systems, allowing to study cell-cell interactions *in vitro* in the present of specific GFs.

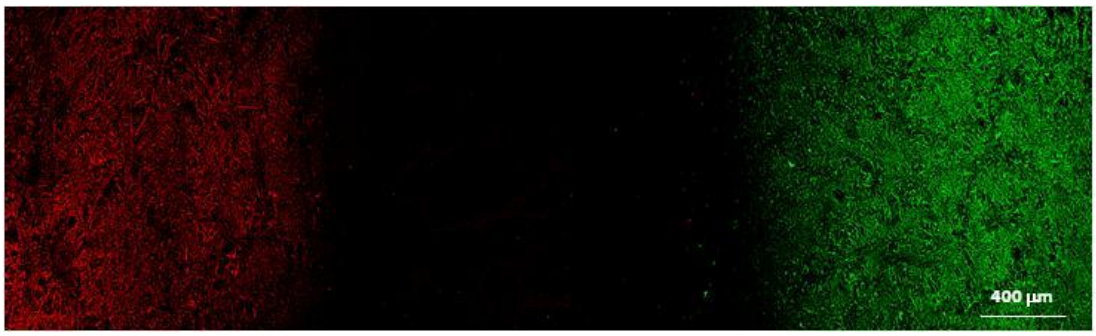

Figure 3.10 Laser scanning confocal microcopy image demonstrating the side-by-side antibodies immobilization over the same activated and functionalized Nanofibrous substrate.

3.4 Conclusions

The covalent immobilization method was successfully implemented in nanofibrous substrates, presenting different efficiencies depending on the antibody of interest. After the antibodies immobilization in different designs, the biofunctionalized nanofibrous substrates enabled the binding of the corresponding growth factors, as well as to select a specific GF from a complex biological fluid (i.e. PLs) comprising a pool of different GFs and proteins. The bioactivity of the bound growth factors was confirmed by cell culture assays, and the beneficial outcomes of the nanofibrous substrate bound GFs were confirmed by biochemical data. The biological data suggests that this substrate offers unique possibilities to study basic cell biology as well as tissue engineering and regenerative medicine fields, since it is possible to specifically bind different GFs of interest at the surface of the nanofibrous substrate. Ultimately, using both biological fluids and cells from an autologous source, it will be possible to implement very effective and personalized therapies tailored for specific clinical conditions.

3.5 References

1. Hildebrand, H. F. *et al.* Functionalization of Biomaterials. *Key Eng. Mater.* 288-289, 47–50 (2005).
2. Carla E. Giacomelli, Laura E. Valenti & Lucrecia Carot. Surface and Colloid Science, 2007
3. Dixit, C. K., Vashist, S. K., MacCraith, B. D. & O'Kennedy, R. Multisubstrate-compatible ELISA procedures for rapid and high-sensitivity immunoassays. *Nat. Protoc.* 6, 439–45 (2011).
4. Feyssa, B. *et al.* Patterned Immobilization of Antibodies within Roll-to-Roll Hot Embossed Polymeric Microfluidic Channels. *PLoS One* 8, e68918 (2013).
5. Pei, Z. *et al.* Optimizing immobilization on two-dimensional carboxyl surface: pH dependence of antibody orientation and antigen binding capacity. *Anal. Biochem.* 398, 161–8 (2010).
6. Peluso, P. *et al.* Optimizing antibody immobilization strategies for the construction of protein microarrays. *Anal. Biochem.* 312, 113–124 (2003).
7. Qian, W. *et al.* Immobilization of antibodies on ultraflat polystyrene surfaces. *Clin. Chem.* 46, 1456–63 (2000).
8. Karyakin, A. A., Presnova, G. V., Rubtsova, M. Y. & Egorov, A. M. Oriented Immobilization of Antibodies onto the Gold Surfaces via Their Native Thiol Groups. *Anal. Chem.* 72, 3805–3811 (2000).
9. Dixit, C. K., Mcdonagh, C., Maccraith, B. D., Biophotonics, N. & Platform, I. Surface Modification and Conjugation Strategies for Bioassay / Biomaterial Applications. (2011).
10. Jung, Y., Jeong, J. Y. & Chung, B. H. Recent advances in immobilization methods of antibodies on solid supports. *Analyst* 133, 697–701 (2008).
11. Zhan, J., Singh, A., Zhang, Z., Huang, L. & Elisseeff, J. H. Multifunctional aliphatic polyester nanofibers for tissue engineering. *Biomatter* 2, 202–12
12. Pham, Q. P., Sharma, U. & Mikos, A. G. Electrospinning of polymeric nanofibers for tissue engineering applications: a review. *Tissue Eng.* 12, 1197–211 (2006).
13. Martins A, Alves da Silva M, Reis RL, N. N. Polymeric mesh with selective permeability, for the repair and regeneration of tissues. PCT/IB2013/056218.
14. Barrientos, S., Stojadinovic, O., Golinko, M. S., Brem, H. & Tomic-Canic, M. Growth factors and cytokines in wound healing. *Wound Repair Regen.* 16, 585–601
15. Krishnamoorthy, L., Morris, H. L. & Harding, K. G. Specific growth factors and the healing of chronic wounds. *J. Wound Care* 10, 173–8 (2001).
16. Grazul-Bilska, A. T. *et al.* Wound healing: the role of growth factors. *Drugs Today (Barc).* 39, 787–800 (2003).
17. Alsousou, J., Thompson, M., Hulley, P., Noble, a & Willett, K. The biology of platelet-rich plasma and its application in trauma and orthopaedic surgery: a review of the literature. *J. Bone Joint Surg. Br.* 91, 987–96 (2009).
18. Anitua, E., Sánchez, M., Prado, R. & Orive, G. Plasma rich in growth factors: the pioneering autologous technology for tissue regeneration. *J. Biomed. Mater. Res. A* 97, 536 (2011).
19. Martins, A. *et al.* Surface modification of electrospun polycaprolactone nanofiber meshes by plasma treatment to enhance biological performance. *Small* 5, 1195–206 (2009).
20. Monteiro N., Martins A., Pires R. A., Faria S., Fonseca N. A., Moreira J. N., Reis R. L., and N. N. M. *Immobilization of bioactive factor-loaded liposomes at the surface of electrospun nanofibers targeting tissue engineering strategies*. (2013). doi:10.1002/term.1822
21. Krump-Konvalinkova, V. *et al.* Generation of Human Pulmonary Microvascular Endothelial Cell Lines. *Lab. Investig.* 81, 1717–1727 (2001).

22. Masters, K. S. Covalent growth factor immobilization strategies for tissue repair and regeneration. *Macromol. Biosci.* 11, 1149–63 (2011).
23. Anitua, E., Prado, R., Sánchez, M. & Orive, G. Platelet-Rich Plasma: Preparation and Formulation. *Oper. Tech. Orthop.* 22, 25–32 (2012).
24. Tang, Y. *et al.* TGF-beta1-induced migration of bone mesenchymal stem cells couples bone resorption with formation. *Nat. Med.* 15, 757–65 (2009).
25. Zhao, L., Jiang, S. & Hantash, B. M. Transforming growth factor beta1 induces osteogenic differentiation of murine bone marrow stromal cells. *Tissue Eng. Part A* 16, 725–33 (2010).
26. Park, H., Temenoff, J. S., Holland, T. A., Tabata, Y. & Mikos, A. G. Delivery of TGF-beta1 and chondrocytes via injectable, biodegradable hydrogels for cartilage tissue engineering applications. *Biomaterials* 26, 7095–103 (2005).
27. Intini, G. The use of platelet-rich plasma in bone reconstruction therapy. *Biomaterials* 30, 4956–66 (2009).
28. Yun, Y.-R. *et al.* Fibroblast growth factors: biology, function, and application for tissue regeneration. *J. Tissue Eng.* 2010, 218142 (2010).
29. Grainger, D., Vo, T. N., Kasper, F. K. & Mikos, A. G. Strategies for controlled delivery of growth factors and cells for bone regeneration. *Adv. Drug Deliv. Rev.* 64, 1292–1309 (2012).
30. Chiu, L. L. Y. & Radisic, M. Scaffolds with covalently immobilized VEGF and Angiopoietin-1 for vascularization of engineered tissues. *Biomaterials* 31, 226–241 (2010).
31. Ferrara, N., Gerber, H.-P. & LeCouter, J. The biology of VEGF and its receptors. *Nat. Med.* 9, 669–76 (2003).
32. Leslie-Barbick, J. E., Moon, J. J. & West, J. L. Covalently-immobilized vascular endothelial growth factor promotes endothelial cell tubulogenesis in poly(ethylene glycol) diacrylate hydrogels. *J. Biomater. Sci. Polym. Ed.* 20, 1763–79 (2009).
33. Sam, S. *et al.* Semiquantitative study of the EDC/NHS activation of acid terminal groups at modified porous silicon surfaces. *Langmuir* 26, 809–14 (2010).
34. Staros, J. V, Wright, R. W. & Swingle, D. M. Enhancement by N-hydroxysulfosuccinimide of water-soluble carbodiimide-mediated coupling reactions. *Anal. Biochem.* 156, 220–2 (1986).
35. Chou, C.-H. *et al.* TGF-beta1 immobilized tri-co-polymer for articular cartilage tissue engineering. *J. Biomed. Mater. Res. B. Appl. Biomater.* 77, 338–48 (2006).
36. Motoyama, M. *et al.* In vitro cartilage formation using TGF-beta-immobilized magnetic beads and mesenchymal stem cell-magnetic bead complexes under magnetic field conditions. *J. Biomed. Mater. Res. A* 92, 196–204 (2010).
37. DeLong, S. A., Moon, J. J. & West, J. L. Covalently immobilized gradients of bFGF on hydrogel scaffolds for directed cell migration. *Biomaterials* 26, 3227–34 (2005).
38. Shen, H., Hu, X., Bei, J. & Wang, S. The immobilization of basic fibroblast growth factor on plasma-treated poly(lactide-co-glycolide). *Biomaterials* 29, 2388–99 (2008).
39. Ma, Z., Gao, C., Gong, Y. & Shen, J. Cartilage tissue engineering PLLA scaffold with surface immobilized collagen and basic fibroblast growth factor. *Biomaterials* 26, 1253–9 (2005).
40. Shen, Y. H., Shoichet, M. S. & Radisic, M. Vascular endothelial growth factor immobilized in collagen scaffold promotes penetration and proliferation of endothelial cells. *Acta Biomater.* 4, 477–89 (2008).
41. Miyagi, Y. *et al.* Biodegradable collagen patch with covalently immobilized VEGF for myocardial repair. *Biomaterials* 32, 1280–90 (2011).
42. Sharon, J. L. & Puleo, D. A. Immobilization of glycoproteins, such as VEGF, on biodegradable substrates. *Acta Biomater.* 4, 1016–23 (2008).

43. Ito, Y., Hasuda, H., Terai, H. & Kitajima, T. Culture of human umbilical vein endothelial cells on immobilized vascular endothelial growth factor. *J. Biomed. Mater. Res. A* 74, 659–65 (2005).
44. Folkman, J. & Haudenschild, C. Angiogenesis in vitro. *Nature* 288, 551–556 (1980).
45. Maciag, T., Cerundolo, J., Ilsley, S., Kelley, P. R. & Forand, R. An endothelial cell growth factor from bovine hypothalamus: identification and partial characterization. *Proc. Natl. Acad. Sci. U. S. A.* 76, 5674–8 (1979).
46. Chiu, L. L. Y., Weisel, R. D., Li, R. & Radisic, M. Defining conditions for covalent immobilization of angiogenic growth factors onto scaffolds for tissue engineering. 69–84 (2011). doi:10.1002/term

Chapter 4 General Conclusions and Future Work

Chapter 4

General Conclusions and Future Work

4.1 General Conclusions

The activation and functionalization of electrospun polycaprolactone (PCL) nanofibers surface allowed the insertion of defined chemical cues, -NH_2 groups, that can react with the COOH from the antibodies forming a stable covalent immobilization. From the optimization study it was possible to optimize the ratio of EDC/NHS and its concentrations, to obtain the maximum immobilization capacity of the nanofibrous substrate.

Different antibodies demonstrated different immobilization densities over the same polymeric substrate. We proposed that the different densities are dependent on the size the antibodies, since higher concentrations of immobilization are obtained with antibodies of lower molecular weight. A standard curve, correlating the different concentrations of each antibody was also obtained demonstrating the linearity of the immobilization method. Confocal microscopy analysis of single antibodies immobilization confirmed that the secondary antibody could specifically link to the immobilized primary antibody, demonstrating the specificity and the efficiency of this methodology. Furthermore, the antibodies immobilization method was effective, since the correspondent growth factors were successfully bound and further quantified. We determined the maximum binding capacity of the recombinant proteins showing that those values stabilize for the maximum concentration of the immobilized antibodies. The amount of PL-derived GFs was determined and, at least, approximately 50% of each GF was selectively bound to its corresponding antibody. The bioactivity of the bound-VEGF (Recombinant and PL-derived) was assessed by seeding and culturing a specific cell line (HPMEC-ST1. R6) over the activated and functionalized nanofibrous substrate. Biological data showed significant differences when bound VEGF (either recombinant or from PLs) was compared to the nanofibrous substrate without VEGF (only the primary antibody immobilized). This observation showed that the VEGF is indeed specifically bound, bioactive and provides beneficial cellular outcomes. Furthermore, the immobilized form of VEGF even showed significant differences when compared to the soluble ECGS supplemented in the culture medium demonstrating that the presence of the GFs at the surface and in the vicinity of the

seeded cells maximizes its bioactivity. With the immobilization of more than one antibody it was possible to assess the selective bound of two different GFs from PLs in a homogenous and mixed distributed form. With the side-by-side immobilization of two antibodies (in this case bFGF and VEGF) the developed watertight chamber system enabled separating the functionalization of a single NFM immobilized with two different antibodies. This strategy allows validating strategies to further design advanced therapies, which combine in a single device various biomolecules enhancing surface functionalization.

4.2 Future Work

This strategy will allow for the immobilization of single or multiple antibodies, and corresponding GFs binding depending on the target applications. It is proposed, as future work, the evaluation of the mixed immobilization of two GFs with complementary roles by assessing their bioactivity and functionality by culturing human mesenchymal stem cells (MSCs), and driving its differentiation into a defined lineage (e.g. osteogenic or chondrogenic). With the side-by-side immobilization strategy it is possible to have two distinct GFs in different areas of the same substrate enabling elucidates its functional role over two distinct cell types. Therefore, the two types of cells (e.g. endothelial/osteoblasts or osteoblasts /chondrocytes) could be seeded over the two distinct areas of the nanofibrous substrate, where a certain antibody and the corresponding GF were previously immobilized. With this strategy it would be possible to obtain tailored co-culture systems, allowing to study GF-mediated cell-cell interactions. To assess the *in vivo* efficiency of the immobilized antibody or bound GF on this nanofibrous substrate, these biofunctionalized substrates will be also studied and its functionality in vivo validated in relevant animal models.

This versatile immobilization strategy can be to transpose to different polymeric substrates currently in use in the clinic, namely bioresorbable devices (i.e. meshes, screws). In particular wound dressing meshes (for diabetic ulcers) or membranes for guided tissue regeneration in the context of dentistry are in the frontline of the translational of this strategy into the clinic.